PAP-700

ROLL WAVES AND SLUG FLOWS IN INCLINED OPEN CHANNELS

by

Dr. Paul G. Mayer, A. M.

Presented at the Seventh National Conference, Hydraulics Division,
American Society of Civil Engineers
Atlanta, Georgia

August 20-22, 1958

ROLL WAVES AND SLUG FLOWS IN INCLINED OPEN CHANNELS

Presented at the Seventh National Conference
Hydraulics Division, American Society of Civil Engineers

Atlanta, Georgia
August 20-22, 1958

by

Dr. Paul G. Mayer, A.M.
Assistant Professor of Civil Engineering
Cornell University, Ithaca, New York

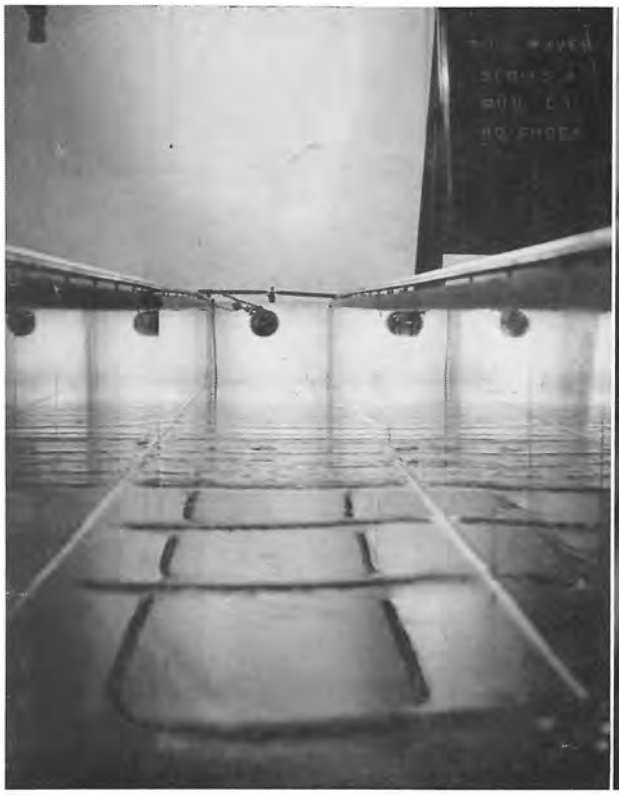

ROLL WAVES

TURBULENT SPOTS

ROLL WAVES AND SLUG FLOWS

INTERMITTENT FLOWS in open channels have long been an unexplained phenomenon. The cause and subsequent development of intermittent surges were investigated. As a result of this investigation, two distinctly different wave train phenomena can be delineated. They are designated respectively as roll waves and slug flows.

Roll waves are the result of the interaction of surface tension and gravity forces at a slightly disturbed surface. They are characterized by transverse ridges of high vorticity and intermittent quiescent zones.

Slug flows result from instabilities which cause the transition from supercritical laminar to turbulent flow. Locally disturbed regions spread transversely and contaminated adjacent zones similar to turbulent spots in wind tunnel investigations. Slug flows are characterized by a succession of highly agitated surges separated by turbulent regions.

The research was carried out by Dr. Paul G. Mayer, Assistant Professor in the Department of Hydraulics and Hydraulic Engineering, School of Civil Engineering, as a laboratory investigation.

NOTATIONS AND DEFINITION OF TERMS

D_i	Depth at point of initiation of disturbance
D_1	Depth of average wave trough
D_h	Depth of average wave crest
D_{1+}	Ratio of depth D_1/D_i
D_{h+}	Ratio of depth D_h/D_i
D_{p+}	Ratio of depth D_p/D_i
X_i	Channel station at point of initiation of disturbance
q	Discharge per unit width
V	Mean velocity
V_s	Surface velocity
V_w	Velocity of roll wave
V_j	Velocity of turbulent spot (jump)
V_{sl}	Velocity of slug (bore)
V_{w+}	Velocity ratio V_w/V_s
V_{j+}	Velocity ratio V_j/V_s
V_{sl+}	Velocity ratio V_{sl}/V_s
ρ	Mass density of water
σ	Surface tension
ν	Kinematic viscosity
f	Frequency of wave
λ	Wave length
N_F	Froude number
R_D	Reynolds number in terms of depth
R_X	Reynolds number in terms of station
N_W	Weber number
S	Channel slope
N_D	Critical depth number
F_{cr}	Critical flow number

All terms are expressed in basic units of the English system.

SYNOPSIS

Roll waves and slug flows are established as two distinctly different wave patterns and are studied phenomenologically in an inclined open channel. The basic characteristics of flow are expressed in terms of pertinent physical properties. A theory is presented and reference is made to similar phenomena in allied fields in which mathematical analyses exist. It is hoped that this study will extend the present knowledge of unsteady phenomena in open channel flow.

INTRODUCTION

Flow in open channels is characterized by a free surface with constant pressure conditions. Possible steady state regimes have been designated conveniently(1) as laminar-subcritical, laminar-supercritical, turbulent-subcritical and turbulent-supercritical. However, unsteady flows exist which are not amenable to analysis by methods applicable to any of the above regimes.

One such unsteady regime occurs in shallow flows in inclined open channels. It is characterized by intermittent surges and wavy patterns and has been variously called roll waves, rain waves, slug flows, and other names. Hydraulic engineers encounter these unsteady flows in inclined open channels and spillways. The increased height of the waves requires additional freeboard to prevent spillage. The concentrated mass of these surges calls for added structural safety factors against transient pressures and stresses. In laboratory studies of hydraulic models, these unsteady flows often interfere with similarity conditions.

To chemical engineers, the phenomena are important in liquid-gas reaction processes. Liquid mass transfer rate is basic to diffision reactions and the rate is greatly increased in unsteady regions.

As a result of this investigation, two distinctly different wave train phenomena can be delineated. They are designated respectively as roll waves and slug flows.

Roll waves are the result of the interaction of surface tensions and gravity forces at a slightly disturbed surface. They are characterized by transverse ridges of high vorticity and intermittent quiescent zones.

Slug flows result from instabilities which cause the transition from supercritical laminar to turbulent flow. Locally disturbed regions spread transversely and contaminated adjacent zones similar to turbulent spots in wind tunnel investigations. Slug flows are characterized by a succession of highly agitated surges separated by turbulent regions.

(1) Numbers refer to reference in bibliography.

THE THEORY OF ROLL WAVES AND SLUG FLOWS

Surface disturbances on a liquid body are due to externally impressed disturbances on amplified internal perturbation. A surface disturbance is subject to both surface and gravity forces.

Fig. 1

When set in motion, capillary and gravity waves result. The general equation for the celerity of surface waves contains expressions for both types.(2)

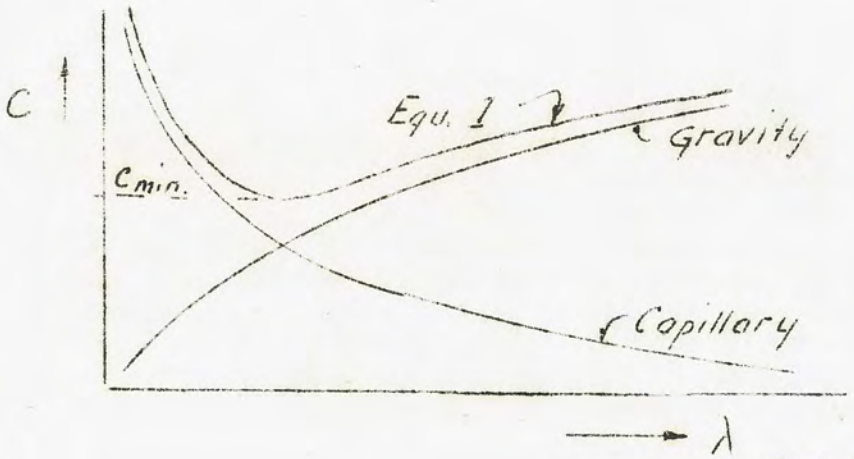

Fig. 2

$$C = \sqrt{\frac{2\pi\sigma}{\lambda\rho} + \frac{\lambda g}{2\pi}} \qquad (1)$$

As indicated in Fig. 2, for waves of short wave length and large curvature, capillary waves predominate. Long waves are predominantly gravity waves and in shallow flows, their celerity approaches $\sqrt{gD}$. Celerity is defined as the wave speed relative to the medium. A minimum celerity exists for surface waves when both influences are equal. $C_{min.}$ is obtained by differentiation of the general wave equation in respect to . Then,

$$C_{min} = \sqrt[4]{\frac{4g\sigma}{\rho}} \qquad (2)$$

and the corresponding wave length is

$$\lambda = 2\pi\sqrt{\frac{\sigma}{\rho g}} \tag{3}$$

When small disturbances are impressed upon a surface, the celerity of each wave is determined uniquely for every wave length. Wave groups are known to travel at speeds different from the celerity of solitary waves. The group velocity of capillary waves is

$$C_{GR.} = \frac{3}{2} C \tag{4}$$

and for gravity waves

$$C_{GR.} = \frac{1}{2} C \tag{5}$$

Both expressions are derived from the general form

$$C_{GR.} = C - C\frac{dC}{d\lambda} \tag{6}$$

In open channel flow with a disturbed surface, both capillary waves and gravity waves exist. Their behavior and the competition between them are responsible for the formation of roll waves and slug flows. Most solutions of instability problems and the analysis of progressive waves are based upon the assumption of parallel flow. In this study, the proximity of the boundary is important and the initially smooth flow suggests viscous flow. For a case of one-dimensional viscous motion, the Navier-Stores equation reduces to

$$0 = \nu\nabla_y^2 + g\sin\theta \tag{7}$$

Assuming a no-slip condition at the fixed boundary

$$v = 0 \quad at \quad y = 0$$

and

$$\mu\frac{dv}{dy} = 0 \quad at \quad y = D$$

Upon integration, the velocity becomes

$$v = \frac{g\sin\theta}{\nu}\left(yD - \frac{y^2}{2}\right) \tag{8}$$

At the surface, y = D, and

$$v = V_s = \frac{g D^2 \sin\theta}{2\nu} \tag{9}$$

This profile is obviously parabolic and the mean stream velocity is

$$V = \tfrac{2}{3} V_s = \frac{g D^2 \sin\theta}{3\nu} \tag{10}$$

For relatively shallow slopes

$$\sin\theta = \tan\theta = S$$

and, hence,

$$V = \frac{g D^2 S}{3\nu} \tag{10a}$$

For progressive waves to form, the following condition must be satisfied

$$V + \sqrt{gD} \geq V_s \tag{11}$$

For laminar flow, a limiting condition exists when an equality is assumed

$$V + \sqrt{gD} = V_s = \tfrac{3}{2} V \tag{12}$$

Subracting from both sides the mean stream velocity and dividing by , the result is

$$1 = \tfrac{1}{2} N_F$$

and

$$N_F = 2 \tag{12a}$$

Interestingly, this critical value of Froude number was also established by M. T. Lighthill and G. B. Whitham[3], who used the Chezy equation in their derivation.

Other significant parameters are the slope and Reynolds number. Using expression 10a, the Reynolds number becomes

$$R_D = \frac{g D^3 S}{3\nu^2} \tag{13}$$

The velocity and depth expressed in terms of Reynolds numbers become

$$V = \left(\frac{gS\nu}{3}\right)^{1/3} R_D^{2/3} \tag{14}$$

and

$$D = \left(\frac{3\nu^2}{gS}\right)^{1/3} R_D^{1/3} \tag{15}$$

The critical Froude number can now be interpreted in terms of a Reynolds number and a slope. From expressions 12a, 14, and 15

$$\frac{1}{2}\left(\frac{gS\nu}{3}\right)^{1/3} R_D^{2/3} = \sqrt{g\left(\frac{3\nu^2}{gS}\right)^{1/3} R_D^{1/3}} \tag{16}$$

Squaring both sides and simplifying, the relationship becomes

$$R_D = \frac{12}{S} \tag{17}$$

and

$$S = \frac{12}{R_D} \tag{17a}$$

Similarly, in laminar flow, the Froude number is

$$N_F = \frac{g D^2 S}{3\nu\sqrt{gD}} \tag{18}$$

and in terms of Reynolds number and slope

$$N_F = \sqrt{\frac{S}{3}}\sqrt{R_D} \tag{19}$$

which again leads at $N_F = 2$ to

$$S = \frac{12}{N_R}$$

As a matter of interest, the critical slope formula by Thomas[4], Dressler[5], Lighthill[6] and others was

$$S = \frac{4g}{C^2}$$

where C was the coefficient of Chezy's formula. Now, the Chezy formula can be expressed for laminar flow as follows

$$V = \frac{gD^2S}{3\nu} = C\sqrt{DS} \tag{20}$$

$$V = g\frac{D^{3/2}S^{1/2}}{3\nu}\sqrt{DS} \qquad (20a)$$

$$V = \sqrt{\frac{g}{3}R_D}\sqrt{DS} \qquad (20b)$$

Hence,

$$C = \sqrt{\frac{g}{3}R_D} \qquad (21)$$

Inserting this coefficient into the critical slope formula gives

$$S = \frac{4g}{C^2} = \frac{4g}{\frac{g}{3}R_D}$$

and significantly,

$$S = \frac{12}{R_D}$$

The behavior of surface disturbances on flows with Froude numbers is

$$N_F \gtrless 2$$

next considered. The criterion was established by assuming the fluid velocity equal to the velocity of a small save so that the profile remains unaltered and the waves cannot break.

If the Froude number is less than $N_F = 2$, the wave velocity exceeds the surface velocity of the stream and

$$V + \sqrt{gD} > V_S$$

The initial disturbances may be sinusoidal pulses, so that both humps and depressions exist. The propagation speed of long waves increases with increases in height. Also, the higher points of a wave profile move with greater speed than lower points.(7) Thus, waves steepen until breaking is imminent (Fig. 3).

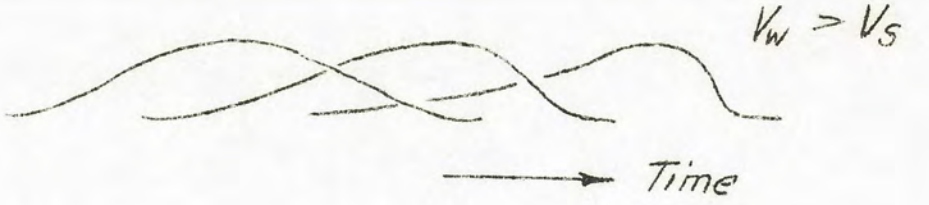

Fig. 3

The increase in curvature brings more surface tension effects into action. Fig. 4 shows how long gravity waves decelerate as capillary forces become important. In the limit, the condition of minimum celerity is attained.

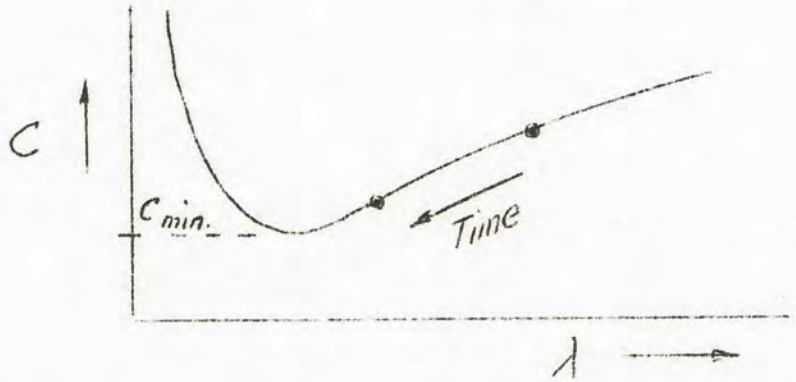

Fig. 4

As the wave length decreases the wave height increases and breaking of progressive waves in shallow water always takes place.

The frontward steepening of gravity waves and the subsequent increase of capillary effects are primarily responsible for roll wave formation. Two possible developments are suggested:

Case 1. Long waves steepen, decelerate, amplify and break. If the resulting waves are influenced equally strong by capillary and gravity forces, a wave train of ripples results which moves continually with a constant velocity.

$$V_w = V + C_{min.}$$

Case 2. When the breaking of the waves takes place, a spectrum of wavelets results. Each in turn is subject to surface and gravity forces. The wavelets are assumed to be of the same height but not necessarily of the same frequency. Since the wavelets may have celerities different from the initial wave, some are assumed to interfere with each other. This interference is similar to the phenomenon of sound waves which have different frequency and phase relations. The resultant of two waves of nearly the same frequency varies in amplitude from zero to twice the amplitude of either component. In the channel, the process of interference may repeat itself until waves of larger amplitude and selected frequency predominate. Finally, the forces of gravity exceed the surface tension effects. The larger waves overtake smaller waves, coalesce with them and grow even larger. After a formative period, roll waves travel independently of each other and approach a terminal velocity (Fig. 5).

When the Froude number is larger than two ($N > 2$), the velocity of a small surface wave is less than the surface velocity of the fluid. The steepening of the wave occurs at the upstream end. The increase in curvature causes a decrease of wave length and a deceleration of the wave, and consequently, the waves break at the upstream end.

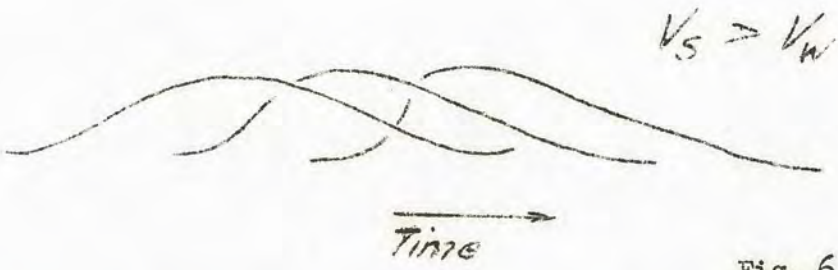

Fig. 6

The subsequent developments are outlined by two hypothesis.

Hypothesis 1. The waves break at the upstream end and the entire stream is affected. Since the wave velocity is less than some fluid velocity, the higher velocity fluid enters a region decelerated by the breaking of the wave. Consequently, the main stream is also decelerated. Some of the kinetic energy is converted into potential energy and the depth of flow increases. Some of the kinetic energy is expended in agitation and mixing. The combined effects are a local hydraulic jump which marks the transition from smooth supercritical flow to highly agitated flow.

Hypothesis 2. The breaking of the wave unbalances the dynamic equilibrium of the supercritical stream which is potentially ready to become turbulent. In laminar supercritical flow on a smooth channel, the breaking of waves triggers the transition to turbulent flow. The change in flow conditions exhibits a sudden increase in resistance to flow. Although the channel slope and the boundary conditions are unaltered, the high velocity flow enters upon a friction slope not sufficient to maintain that velocity and a hydraulic jump occurs.

Subsequently, the agitated region grows into adjacent undisturbed flow. The velocity distribution in each regime is different and mixing takes place. Vorticity transport and turbulent agitation cause lateral contamination. The jump front is maintained as long as it is fed energy by the entering high velocity stream (Fig. 7). When an earlier jump intercepts this high velocity stream, the jump front remains a negative bore until all available energy is fed into it. Then the jump decays and forms an expansion wave and the downstream face of the disturbed region becomes a positive bore. Subsequent bores telescope and form the characteristic saw-tooth profile of slug flows (Figs. 8 and 9).

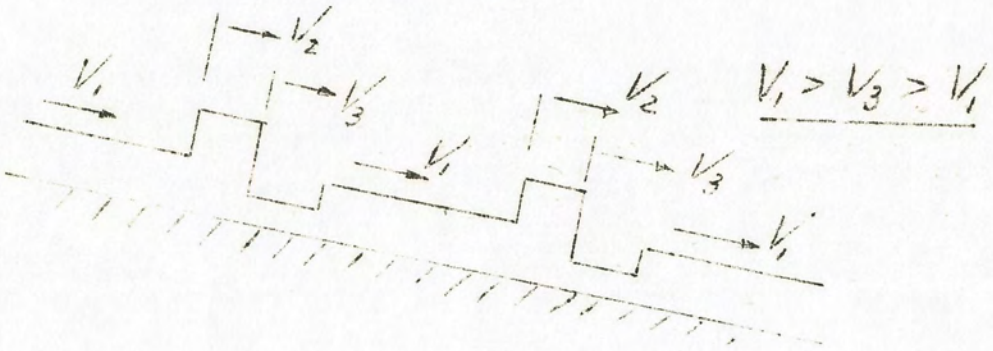

Fig. 7

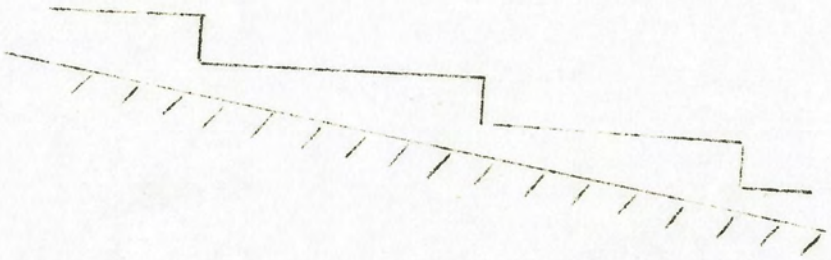

Fig. 8

LABORATORY EXPERIMENTS

Rigorous mathematical treatment of complex hydraulic phenomena encounters great difficulties. Convenient approximations often lead to equations of questionable veracity. The background of experimental reality provides important insight into physical phenomena. Interpretive physical reasoning and dimensional analysis are other tools important to an investigator.

The pertinent variables of a hydraulic phenomenon may be categorized into:

a) boundary conditions,
b) kinematic and dynamic flow characteristics,
c) fluid properties.

A general equation of flow may be written such that a function of all the variables is set equal to zero. Then, suitable power products of the variables can be grouped into dimensionless parameters.(8) Quantities pertinent to the initiation and subsequent development of roll waves and slug flows were:

D_o, depth upstream from disturbance
D_i, depth at point of initiation of disturbance
D_l, depth of average wave trough
D_h, depth of average wave crest
D_p, depth of peak crest
X, channel station at point of initiation
S, slope of channel
q, volume rate of flow per unit width
V_s, surface velocity of water
V_w, velocity of roll wave
V_j, velocity of traveling hydraulic jump (turbulent spot)
V_{sl}, velocity of slug flow
ρ, mass density of water
σ, surface tension
ν, kinematic viscosity
f, frequency of wave
λ, wave length

All quantities are expressed in basic dimensions of the English system. The flow characteristics and boundary conditions were measured in the laboratory. Fluid properties were taken from appropriate tables.

Laboratory Equipment

Apparatus used in this experiment included the test flume; equipment to measure discharge, depth, and velocity; a disturbance generator; and photographic equipment. Some of the apparatus was assembled by the author with this specific investigation in mind. Other equipment was existent and modified.

The experimental work was carried out with a tiltable flume (Fig. 10). The channel consisted of two sections. Each section was 12 feet long, 18 inches wide, and 12 inches deep. The channel floor was covered by two 12 foot long slabs of 1/4 inch thick plate glass. The side walls, also of plate glass, were installed in 4 foot sections. The underside of the floor slabs were painted black. The side walls were left clear. All longitudinal and transverse joints were cast with paraffin and planed down to perfect joint conditions.

The tilting of the channel was accomplished by adjusting the various jacks manually.

Water entered the test flume through a 3-1/2 by 2 by 1-1/2 foot head tank. Wire screens were placed in the tank which supported a graded gravel and sand layer four inches thick. This filter course was intended to reduce the initial turbulence in the flow. A curved steel section extended into the stilling basin. It was aligned with the glass bottom in order to obtain smooth entrance conditions. The top members of the channel frame served as supports for continuous brass rails of 3/4 inch diameter. This track facilitated the quick and easy movement of an instrument carriage. The channel was marked in one foot stations, commencing at the crest.

The water supply was measured by a series of three float type variable area flow meters. Their respective effective ranges were:

a) from 0.001 cfs/ft. to 0.006 cfs/ft.
b) from 0.005 cfs/ft. to 0.030 cfs/ft.
c) from 0.010 cfs/ft. to 0.060 cfs/ft.

These meters had been calibrated and were checked intermittently by collecting the flow for gravimetric measurements. A Toledo dial type platform scale was used. All water was subsequently wasted.

Depth measurements under steady flow conditions were made with a point gage. This gage was mounted on the instrument carriage. For greater accuracy, an attached Federal dial indicator allowed readings to 0.001 inches.

For depth measurements in wavy and unsteady flows, the variations in height were recorded by the electronic wave recorder. The primary component of this consisted of two 0.005 inch thick platinum probes separated by a distance of about sixteen millimeters (5/8 inch). The passing water acted as the electrolyte. The signal was amplified in the wave height measuring device. This amplifier had been built by the Instrumentation Branch of the U. S. Army Corps of Engineers, Waterways Experimentation Station, Vicksburg, Mississippi. A direct writing Brush oscillograph recorded the variations in depth (Fig. 11). The oscillograph records were readily converted into depth measurements with the aid of a calibration curve. The accuracy and reproducability of the electronic measurements were most satisfactory. The Brush oscillograph could be operated at three different speeds; 5 mm./sec., 25 mm./sec., and 12.5 cm./sec. The slowest speed was generally used to measure wave heights and frequencies. The faster speeds were more able to show wave profiles.

For the determination of surface velocities and wave velocities, the time measurements were accomplished with an electric clock capable of recording 0.01 sec. The clock was activated manually be means of a micro-switch. The switch was attached to a long extension chord and thus permitted utmost mobility. The channel stationing was used for length measurements.

A small bottle of compressed gas was attached to the head wall of the stilling basin. A flexible hose connected the bottle to a control valve located in the head wall below the water surface. The rate of release of gas bubbles could also be regulated by the valve attached to the gas container.

All pictures were taken by the author with a Kodak Graphic View camera. Royal Pan 4 by 5 inch sheet film was used exclusively.

Laboratory Procedures

The laboratory procedures evolved during a period of preliminary work. Necessary precautions were detected early and followed in subsequent experiments. Precursory investigations delineated the ranges of slope and discharge within which satisfactory measurements could be taken. All pertinent channel and flow characteristics were observed and recorded repeatedly.

Five different channel slopes were used. Their respective tangents were 0.0175, 0.0349, 0.0524, 0.0699, and 0.0875. On each slope, a series of nine discharges was investigated which ranged from 0.001 cfs/ft. to 0.06 cfs/ft. After the channel slope was set and a given discharge obtained, the instrument carriage was moved from station to station. Considerable time was allowed to elapse after each movement of the carriage in order to eliminate external disturbances as far as possible. Depth measurements and wave recordings were then made. Test results obtained under these conditions were recorded as Regime "Q" (quiescent).

The mean velocity of the flowing water was calculated from the known conditions of discharge and depth. Surface velocities were measured by allowing specks of talcum powder to travel betweer given stations and by measruing elapsed time. This process was repeated four or more times for each measurement.

Wave velocities were established by measuring the time interval in which a wave crest moved between predetermined stations.

The entire sequence of measurements was repeated with the disturbance generator in operation. Test results under these conditions were reported as Regime "S" (shock).

The initial location, type, and subsequent development of the surface disturbances were observed and recorded for every setting of slope and discharge as well as Regime "Q" and Regime "S". Photographs of significant events were taken. Best photographic effects were obtained by indirect lighting. Thus, waves appear in most photographs as shadows.

The water temperatures were measured both in the entrance tank and at the discharge end.

RESULTS OF EXPERIMENTS

The presentation and analysis of the experimental results is best accomplished by a subdivision of the material into a logical sequence. First, the flow conditions leading to instability are discussed. Then, roll wave and slug flow characteristics are presented.

DISCUSSION OF INSTABILITY

Unstable Flows Leading to Roll Wave Formation

In the experimental flume, perfectly smooth laminar sheet flow degenerated into a flow marked by transverse ridges. The instability occurred in a flow which was initially undisturbed. It can be attributed to the natural mode of oscillations inherent in the flow. The same physical results were obtained by the superposition of finite disturbances by means of the disturbance generator. The distinctive difference between the operating conditions was that the breakdown of the flow took place further upstream when finite disturbances were externally impressed.

External disturbances of various amplitudes and frequencies were used. Both factors seemed to bear upon the stability phenomenon. However, the breakdown occurred sooner with larger amplitudes. No quantitative measurements of the disturbance amplitudes or frequencies were made. Significantly, the instability of flow, and hence the formation of roll waves, was eliminated when a wetting agent was added to the water. A wetting agent may affect not only the surface tension of the liquid but also cohesion and spreading. Since spreading of a liquid on a solid surface takes place when the work of adhesion exceeds that of cohesion, an interrelationship exists between surface tension, cohesion, and spreading.(9) The exact action of a specific wetting agent upon the behavior of a liquid in motion requires considerably more study.

The reduction of surface tension eliminated an essential agent for the formation of roll waves. The fact that instability of flow and formation of roll waves were not observed when a wetting agent was added to the fluid is helpful to hydraulicians engaged in model work.

After the breakdown of the laminar flow was precipitated, the development of roll waves proceeded identically, regardless of the mechanism which caused the instability of flow. Hence, laminar flow in inclined open channels was unstable because of inherent disturbances as well as externally impressed perturbations. Surface tension played an important role.

Unstable Flow Leading to Slug Flow Formation

Instability leading to the formation of slug flows is more properly described as the transition from laminar to turbulent flow. Instantaneous point disturbances occurred randomly in the smooth sheet. The disturbed regions spread transversely and were swept downstream at the same time. The photograph on the frontice piece shows this phenomenon. The highly agitated regions differentiated the turbulent flow from the surroudning stream. The nature of these agitated zones was similar to oblique traveling hydraulic jumps. In the literature of aerodynamics, these transitions are known as turbulent spots.(10)

Superimposed disturbances from the disturbance generator had no appreciable effects upon the stability of the flow. However, raindrops onto the channel and sand grains in the channel precipitated turbulent spots. The addition of a wetting agent to the water had no detectable effect upon the flow stability.

Analysis of Experimental Data of Initiation Conditions

Pertinent boundary and flow characteristics of the undisturbed flow prior to the breakdown were grouped into the following five dimensionless parameters:

Depth Reynolds Number,	q/ν	, R_D	(22)
Length Reynolds Number,	$\frac{VX_i}{\nu}$	, R_X	(23)
Froude Number,	$V/\sqrt{gD}$	, N_F	(24)
Weber Number,	$\frac{\rho V^2 D}{T}$	, N_W	(25)
Slope,	$\sin\theta \sim \tan\theta$,	S	(26)

In the presentation of the various characteristic curves, specific symbols were selected to represent certain flow conditions. A legend of the symbols and their meaning is given below:

○ , ripple flow, a train of small waves with short wave length,

△ , roll waves,

✳ , slug flows,

-○- , confused pattern,

+ , agitated turbulent flow, usually at high Reynolds numbers. $R_D > 4000$,

-△- , roll waves at verge of breakdown, usually at $R_D \approx 420$.

A plot of Froude numbers and Reynolds numbers is presented in Fig. 12 with the slope as the third parameter. An analogous relationship was obtained when the gravitational and the surface forces were compared (Fig. 13). The transitional character of these curves is obvious. The graphs on Figs. 12 and 13 show that the surface tension and viscous effects predominated in the phenomenon of roll wave formation. At higher Reynolds numbers, corresponding to the conditions which led to slug flows, viscous and surface tension effects decreased and, finally, became negligible.

From the theoretical considerations, it was seen that the mean velocity and the depth of flow were a function of the slope. Thus, a simplified parameter, the modified Froude number, $N_F/\sqrt{S}$, and the Reynolds number could be plotted into a single curve (Fig. 14). Similar conditions led to a single representation of Froude number, Weber number, and slope (Fig. 15).

A combination of all parameters was undertaken so that an overall grasp of the instability phenomenon might be obtained. This also has practical engineering importance. In practical problems, one may know the conditions of slope, discharge, and temperature. Hence, a parameter exclusive of the depth was plotted against a parameter which was a function of depth, slope, and temperature. The dimensionless parameter containing the rate of flow, q, was named "critical flow number", F_{cr}, the one containing the depth of flow, D, was named "critical depth number", N_D. The derivation of these parameters is shown below.

The instability condition was considered a function of R_D, N_F, N_W, and slope. Thus,

$$0 = \phi\left[R_D, N_W, N_F, S\right] \tag{27}$$

which is identical to:

$$0 = \phi\left[\frac{q}{\nu}, \frac{\rho q^2}{\sigma D}, \frac{q}{\sqrt{g D^3}}, S\right] \tag{28}$$

In order to find the "critical flow number", F_{cr}, the depth was eliminated between the Weber number and the modified Froude number.

$$F_{cr} = f\left[q, S, T\right] = \left(\frac{N_W}{\sqrt{S}}\right)^{3/2}\left(\frac{N_F}{\sqrt{S}}\right)^{-1}$$

$$F_{cr} = q^2\left(\frac{\rho}{\sigma}\right)^{3/2} g^{1/2} S^{-1/4}$$

$$F_{cr} = \left(\frac{\rho q}{\sigma}\,\frac{V^{1/3}(gD)^{1/3}}{S^{1/6}}\right)^{3/2}$$

$$F_{cr} = \left(\frac{\rho q V}{\sigma S^{1/6}}\right)^{3/2} \tag{29}$$

In order to find the critical depth number, N_D, the volume rate of flow was eliminated between the Reynolds number and the modified Froude number.

$$N_D = f(D, S, T) = R_D \left(\frac{N_F}{\sqrt{S}}\right)^{-1} \qquad (30)$$

$$N_D = D^{3/2} (gS)^{1/2} \nu^{-1}$$

$$N_D = \left(\frac{g D^3 S}{\nu^2}\right)^{1/2} \qquad (31)$$

The plot of F_{cr} and N_D is presented in Fig. 16. In the region of instability which led to the formation of roll waves, the two parameters showed a straight line relationship. A mathematical formulation was possible below a $F_{cr} = 4$. The equation was:

$$N_D = 28.1 F_{cr}^{.218} \qquad (32)$$

The Meaning of F_{cr} and N_D

The "critical flow number" simply states that instability is imminent whenever the surface tension forces became comparable in magnitude to the momentum carried by the stream. This is equivalent to saying that the free surface energy becomes comparable to intrinsic energy of the stream.

The "critical depth number" is essentially a Reynolds number for laminar flow. The expression was developed earlier and given as equation 28. A Reynolds number may also be written as:

$$R_D = \frac{VD\rho}{\nu} = \frac{\rho V^2}{\mu V/D} \qquad (33)$$

which expresses the ratio of kinetic energy in the stream to the energy dissipated by viscous shear. Thus, the parameters, F_{cr} and N_D, have perfectly sound physical interpretations.

Experimental Relationship Between Reynolds Number, Froude Number, and Slope

Theoretical considerations predicted definite relationships of the above parameters when a parabolic velocity distribution was assumed. All experimental data were plotted in Fig. 17 to show the general interrelationships. The instabilities which led to the formation of roll waves were in the region of supercritical laminar flow as predicted. Some instabilities leading to slug flows satisfied the predicted conditions, but most data indicated that slug flows were a transitional phenomenon and the actual velocity distribution may have been different.

Equations 17a and 19 predicted that:

$$S_{crit.} = \frac{12}{R_D}$$

$$N_F = \sqrt{S/3}\ \sqrt{R_0}$$

Roll waves were observed up to Reynolds numbers of 410, 413, 419, and 418. The, for a mean $R_{D_{max}} = 415$, the minimum slope for the formation of roll waves was, according to 17a:

$$S_{min} = .029 \sim 3\%$$

which was verified by the experimental results. The corresponding Froude number was experimentally equal to $N_F = 2.06$. At the higher Reynolds numbers, the flow often degenerated into turbulent spots below the overflow entrance to the flume, before uniform flow conditions were obtained. Instabilities which led to the formation of slug flows were usually observed at Reynolds numbers larger than 1250. Turbulent spots were produced below this value by artificial rainfall. The deviation from the theoretical curve (Fig. 18) also starts at a Reynolds number of 1250. With a theoretical minimum Froude number of $N_F = 2$ and an approximate lower limit of Reynolds numbers of 1200, the minimum channel slope for the formation of slug flows is:

$$S = .01$$

Actually, slug flows were observed experimentally on a slope of:

$$S = .0175 \sim 2\%$$

All Froude numbers of flows leading to the formation of slug flows were above the theoretical minimum $N_F = 2$.

Location of Initial Surface Instability

It was observed that the location of the initial disturbances leading to roll wave formation moved downstream with increasing Reynolds numbers. An opposite trend was apparent with slug flows. A plot of the "length Reynolds number" and the "depth Reynolds number" elucidates this phenomenon (Fig. 19).

The plot does not reflect the locations of instability for artificially disturbed flows. Finite disturbances from the generator caused the instabilities to occur further upstream in the case of roll waves. For slug flows, the effect of the generator was less pronounced. Whenever the Froude number was in excess of the theoretical minimum of $N_F = 2$, turbulent spots could be brought about by raindrops onto the channel or by roughening the channel bed with sand grains.

A prediction of the location of the initial surface disturbances cannot be made accurately for channels with entrance conditions and channel linings different from those of the experimental flume.

The Formation of Roll Waves

The flow in the inclined open channel remained undisturbed on slopes up to approximately 1%. Surface disturbances in the form of ripple flow occurred on all tested slopes. Ripple flow was characterized by transverse ridges of short wave length. The speed of these waves was always larger than the surface velocity and equal to:

$$V_w = V + C_{min}$$

where the minimum celerity, $c_{min.}$, under experimental conditions was:

$$C_{min} = .763 \text{ ft./sec.}$$

At conditions not sufficient to form roll waves, the ripple flow continued downstream over the entire length of the test flume.

Roll waves did not form on slopes below 3%. The formation of roll waves is shown schematically on Fig. 20. Perfectly smooth laminar sheet flow first suffered very slight undulations. A breakdown of the flow into ripple flow followed immediately. Then, a confused zone of rearrangement preceded the final emergence of roll waves. The frontice piece shows a photograph of this process. Roll waves were characterized by transverse ridges of high vorticity. The zones between the wave crests remained quiescent.

The Formation of Slug Flows

Slug flows originated with local disturbances. The agitated regions spread transversely and were swept downstream at the same time. A schematic representation of spot growth is shown in Fig. 21. A comparison was made between the experimental results of wind tunnel investigations and the development of the disturbed regions in the inclined open channel. The envelopes of spot growth behaved similarly for Schubauer and Klebanoff's[11] wind tunnel measurements and Amein's[12] result in the test flume (Fig. 22).

The regions between the spots were quiescent. The upstream front of the disturbed regions moved with a velocity approximately equal to 50% of the undisturbed surface velocity, the downstream front at about 80%. The upstream front resembled a traveling oblique hydraulic jump; the downstream end developed into a bore. Slug flows resulted when the quiescent pockets were eliminated by successive bores which telescoped to form the characteristic saw-tooth profile.

Initially smooth water was pierced by occasional bursts of turbulence. The spot incidence increased as the flow progressed downstream. An increase

in spot frequency was also observed with increasing Reynolds numbers. The disturbed regions grew as previously described. A drawdown of the water surface corresponded to a decrease in flow. This observation corresponded to the "slackening" of the current reported by Cornish(13) half a century ago.

Slug flows were characterized by highly turbulent intermittent surges. Transverse ridges separated the regions of agitated flows and numerous smaller waves were seen to ride the larger surges. During the formative period, some waves were reflected from the side walls and could be seen as curved wave fronts. Eventually, the waves coalesced into a common transverse ridge.

Wave Characteristics

For roll waves, the characteristics of wave length, wave height, and velocity were investigated. A comparison of the data of wave height and wave velocity showed that a terminal roll wave velocity existed. The relationship is plotted in Fig. 23. The terminal velocity was then related to channel slope and Reynolds number. Fig. 24 shows the data fitted to a curve and, on a log - log plot, the resulting equation was:

$$\text{Terminal } V_w = .44\, R_D^{1/3}\, S^{1/6} \qquad (60)$$

On the same graph, the surface velocities were superimposed. It was seen that roll waves always travel faster than the undisturbed upstream surface velocity.

The roll wave characteristic described above was dimensional in nature. The orderlines suggested that a dimensional analysis might be profitable. In the following analysis, both roll waves and slug flows were treated alike. Pertinent flow and wave characteristics were grouped into the following dimensionless parameters:

Reynolds number,	R_D
Froude number,	N_F
Dimensionless roll wave velocity,	V_{w+}
Dimensionless slug flow velocity,	$V_{sl.+}$
Depth ratios,	D_{l+}, D_{h+}
Wave height - wave length ratio,	D_h/λ
Wave number,	V_w^2/gq

The physical meaning of the wave number can be interpreted as "kinetic energy per wave per unit discharge". In the presentation of the graphs, the usual symbols were employed.

Fig. 24 already pointed out that the roll wave velocities exceeded the surface velocities, and the terminal velocities were shown to be related to Reynolds number to the one-third power. A plot of dimensionless velocities and Reynolds number showed the same trend for roll waves, but for slug flows, the velocities were always less than the surface velocities, and, in dimensionless form, showed a constant ratio independent of Reynolds number (Fig. 25).

When all the experimental data was plotted in terms of the modified wave number and the ratio of wave height to wave length, a narrow region delineated the zone of wave formation. The data pertaining to the steeper slopes plotted at the lower portion of the loop, so that the characteristics of roll waves and slug flows on still steeper slopes can be fairly well predicted (Fig. 26).

The plot involving the wave number pointed to the fact that this parameter tends to zero with increasing discharge. Slug flows were characteristic at larger discharges and plotted below wave numbers pertaining to roll waves. At very large discharges, the wave number vanishes. This reflects the fact that roll waves and slug flows are phenomena observed only at relatively low discharges. Although the continued growth of wave height and wave length made the length of the experimental channel seem insufficient, the ratio of wave height to wave length approached a limiting value (Fig. 26).

CONCLUSIONS

Steady flows in inclined open channels degenerated into periodic wave patterns under specific conditions of slope and discharge. The sources of instability were either carried by the stream or were externally superimposed perturbations. Two distinct types of wave trains were delineated. They were designated as roll waves and slug flows respectively.

Roll waves formed whenever the surface velocity of the undisturbed stream was less than the minimum velocity of surface waves, provided that the channel slope was sufficiently steep. Experimentally and analytically, the minimum slope sufficient for roll wave formation was about 3%. The maximum Reynolds number of the undisturbed stream was 420. Roll waves resulted from the interaction of surface tension and gravity forces at a slightly disturbed surface. They were characterized by transverse ridges of high vorticity. The regions between the crests were quiescent. The terminal velocities of roll waves were in excess of the surface velocity of the undisturbed stream. The ratio of wave height to wave length approached the limiting value of 0.004.

Slug flows resulted from instabilities which caused the transition from supercritical laminar flow to turbulent flow. The initial disturbances were carried by the stream or resulted from interference by the side walls. The transition was a random phenomenon and could not be ascribed to any partic-

Fig. 24 already pointed out that the roll wave velocities exceeded the surface velocities, and the terminal velocities were shown to be related to Reynolds number to the one-third power. A plot of dimensionless velocities and Reynolds number showed the same trend for roll waves, but for slug flows, the velocities were always less than the surface velocities, and, in dimensionless form, showed a constant ratio independent of Reynolds number (Fig. 25).

When all the experimental data was plotted in terms of the modified wave number and the ratio of wave height to wave length, a narrow region delineated the zone of wave formation. The data pertaining to the steeper slopes plotted at the lower portion of the loop, so that the characteristics of roll waves and slug flows on still steeper slopes can be fairly well predicted (Fig. 26).

The plot involving the wave number pointed to the fact that this parameter tends to zero with increasing discharge. Slug flows were characteristic at larger discharges and plotted below wave numbers pertaining to roll waves. At very large discharges, the wave number vanishes. This reflects the fact that roll waves and slug flows are phenomena observed only at relatively low discharges. Although the continued growth of wave height and wave length made the length of the experimental channel seem insufficient, the ratio of wave height to wave length approached a limiting value (Fig. 26).

CONCLUSIONS

Steady flows in inclined open channels degenerated into periodic wave patterns under specific conditions of slope and discharge. The sources of instability were either carried by the stream or were externally superimposed perturbations. Two distinct types of wave trains were delineated. They were designated as roll waves and slug flows respectively.

Roll waves formed whenever the surface velocity of the undisturbed stream was less than the minimum velocity of surface waves, provided that the channel slope was sufficiently steep. Experimentally and analytically, the minimum slope sufficient for roll wave formation was about 3%. The maximum Reynolds number of the undisturbed stream was 420. Roll waves resulted from the interaction of surface tension and gravity forces at a slightly disturbed surface. They were characterized by transverse ridges of high vorticity. The regions between the crests were quiescent. The terminal velocities of roll waves were in excess of the surface velocity of the undisturbed stream. The ratio of wave height to wave length approached the limiting value of 0.004.

Slug flows resulted from instabilities which caused the transition from supercritical laminar flow to turbulent flow. The initial disturbances were carried by the stream or resulted from interference by the side walls. The transition was a random phenomenon and could not be ascribed to any partic-

ular boundary condition. Locally disturbed regions spread transversely and contaminated adjacent zones. They were swept downstream like traveling oblique hydraulic jumps and seemed analogous to the turbulent spots of boundary layer studies in wind tunnels.

The phenomenon of the "traveling oblique hydraulic jumps" represented a discontinuity in open channel flow. In wind tunnel investigations, the turbulent spots were not considered to be "shock" waves. Although one may consider shallow flow in an inclined open channel a boundary layer phenomenon, the additional force components of gravity and surface tension prohibit a quantitative analogy between compressible and incompressible fluid flows.

Slug flows formed whenever the surface velocity of the undisturbed flow was in excess of the minimum velocity of surface waves. They were characterized by a succession of highly turbulent surges. The wave crests were separated by agitated regions. The terminal velocity of slug flows was less than the surface velocity of the undisturbed stream. The range of Reynolds numbers was from approximately 1200 to below 4000. At Reynolds numbers of 4000, the resulting flow was thoroughly turbulent and no slug flows were observed. The minimum slope for slug flow formation was approximately 2%. The Froude numbers were always in excess of 2. The flow decreased noticeably between waves and the surges literally jumped off the experimental flume.

During particular test runs, not all waves were of the same size or traveled with the same speed. The deviations from the mean were at times considerable and the concept of waves "that are alike in size and shape and travel with a constant velocity" which was expressed by Thomas, Dressler, and other writers must be questioned. In this study, the analysis of the oscillographs as well as the measurements of wave velocity reflect average values.

Roll waves and slug flows were analyzed and plotted in terms of pertinent dimensionless parameters. Flow conditions susceptible to instability were delineated by a "critical depth number" and a "critical flow number". Significant wave characteristics were expressed by a "wave number".

Roughened boundary conditions enhanced the formation of roll waves. Rain waves, the phenomenon often observed on fairly rough street surfaces, are essentially roll waves, and it seems that they will form, regardless of the boundary conditions. Experimentally, slug flows were also precipitated by boundary roughnesses. However, the disturbance sources were isolated three-dimensional obstructions (sand grains). A sufficiently large number of disturbance sources, that is, a very rough channel, agitates the flow sufficiently that slug flows cannot form. This seems to be substantiated by the fact that slug flows are only observed in man-made channels and are not characteristic of swift mountain streams. The roughening of the channel as a measure to eliminate slug flows was pointed out by H. Rouse.(14)

The theory of roll waves and slug flows presented in this study presupposed that the velocity distribution was significant. A parabolic distribution was assumed and was found quite satisfactory. Jeffreys[15] reported earlier that slug flows (alias roll waves) were the transition from "turbulent flow with a nearly plane surface to turbulent flow marked by transverse ridges".

The pertinent characteristics of roll waves and slug flows were expressed in terms of dimensionless parameters. In order to test their validity, a similar study could be undertaken with a different fluid. A longer channel capable of steeper slopes would also extend the range of this study.

Disturbances leading to the formation of roll waves could be superimposed upon the laminar stream by controlled means. In the experiments, randomly generated disturbances led to the same periodic wave formation with the same selected frequency that evolved when an undisturbed stream degenerated into roll waves. The frequencies and amplitudes preferentially leading to roll wave formation could be studied by means of a vibrating ribbon or controlled electric pulses. Similar methods have been employed successfully in wind tunnel studies.

Slug flows were reported to lead to air entrainment on dam spillways. R. Maistre and R. Oblensky[16] published photographs which suggested that air entrainment was caused by surface roughness. Thus, it seems incongruous that rough channels eliminate slug flows but generate air entrainment, if air entrainment is preceded by the former. Further study could delineate the proper significance of the two phenomena in respect to each other.

Theoretical considerations led to a critical Froude number equal to 2. Lighthill and Whitham as well as other writers arrived at the same criterion by different approaches. Under conditions of minimum slope, the Froude number of 2 was the upper limit for roll waves and the lower limit for slug flows. Since slug flows were essentially the transition from supercritical laminar flow to turbulent flow, the significance of the Froude number equal to 2 in terms of laminar-turbulent transition remains to be investigated.

ACKNOWLEDGEMENTS

The author acknowledges gratefully the constructive criticism and kind encouragement by the late Professor Andre L. Jorissen, M. ASCE. Professor Melvin Priest, M. ASCE, suggested the study. Useful suggestions and references were contributed by Dr. L. Crabtree, Cambridge, England, while the latter was at the Graduate School of Aeronautical Engineering of Cornell University.

REFERENCES

(1) Robertson, J. M., and Rouse, H., "On the Four Regimes of Open-Channel Flow", Civil Engineering, II: 169-171, 1940.

(2) Lamb, H., Sir, Hydrodynamics, New York, Dover Publications, 1945.

(3) Lighthill, M. J., and Whitham, G. B., "On Kinematic Waves. I. Flood Movement in Long Rivers", Royal Society of London, Proceedings, 229A: 281-316, May, 1955.

(4) Thomas, H. A., "The Propagation of Waves in Steep Prismatic Conduits", Proceedings of Hydraulic Conference, Iowa City, Iowa, 214-29, 1940.

(5) Dressler, Robert F., "Mathematical Solution of the Problem of Roll-Waves in Inclined Open Channels", Communications on Pure and Applied Mathematics, 2: 149-94, 1949.

(6) Lighthill, M. J., and Whitham, G. B., op. cit.

(7) Stoker, J. J., "The Formation of Breakers and Bore, The Theory of Nonlinear Wave Propagation in Shallow Water and Open Channels", Communications on Applied Mathematics, 1: 1-87, 1948.

(8) Birkhoff, G., Hydrodynamics, New York, Dover Publications, 1955.

(9) Harkins, W. D., The Physical Chemistry of Surface Films, New York, Reinhold Publishing Corporation, 1952.

(10) Emmons, H. W., "The Laminar-Turbulent Transition in a Boundary Layer - Part I", Journal of the Aeronautical Sciences, 18: 490-98, 1951.

(11) Schubauer, G. B., and Klebanoff, P. S., "Contributions on the Mechanics of Boundary Layer Transition", NACA Technical Note 3489, 1955.

(12) Amein, A. M., "Free Surface Disturbances Initiated at the Sides in Steep Open Channels", Unpublished Doctoral Thesis, Cornell University, Ithaca, New York, 1954.

(13) Cornish, V., Waves of the Sea and Other Water Waves, Chapter XI, London, T. Fisher Unwin, 1910.

(14) Rouse, H., Fluid Mechanics for Hydraulic Engineers, New York, McGraw-Hill, 1938.

(15) Jeffreys, Harold, "The Flow of Water in an Inclined Channel of Rectangular Section", Philosophical Magazine and Journal of Science, 49: 793-807, 1925.

(16) Maistre, R., and Oblensky, R., "Etude de Quelques Caracteristiques de l'Ecoulement dans la Partie Avale des Evacuateurs de Surface", La Houille Blanche, Juillet - Aout, 1954, pp. 481-511.

(17) Mayer, P. G., "A Study of Roll Waves and Slug Flows in an Inclined Open Channel", Ph.D. Thesis, Cornell University, Ithaca, New York, 1957.

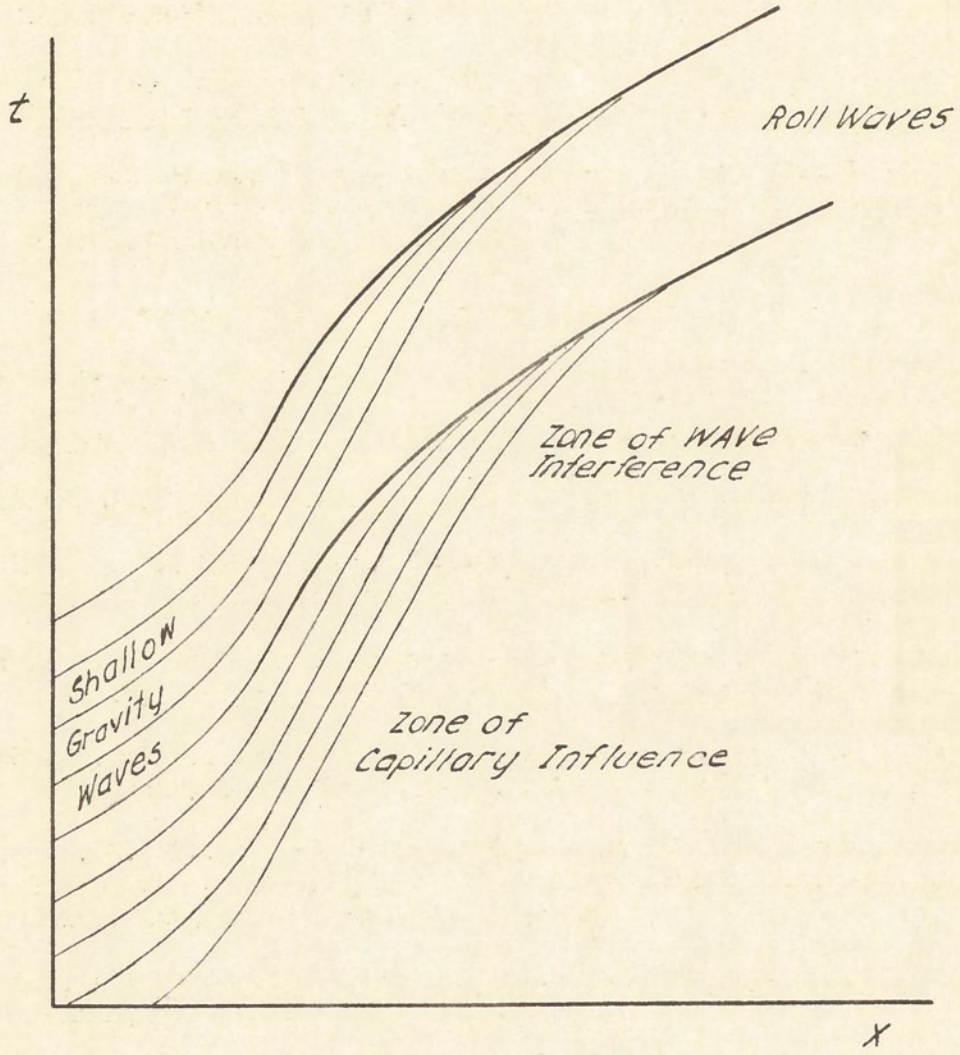

Fig. 5 Development of Roll Waves

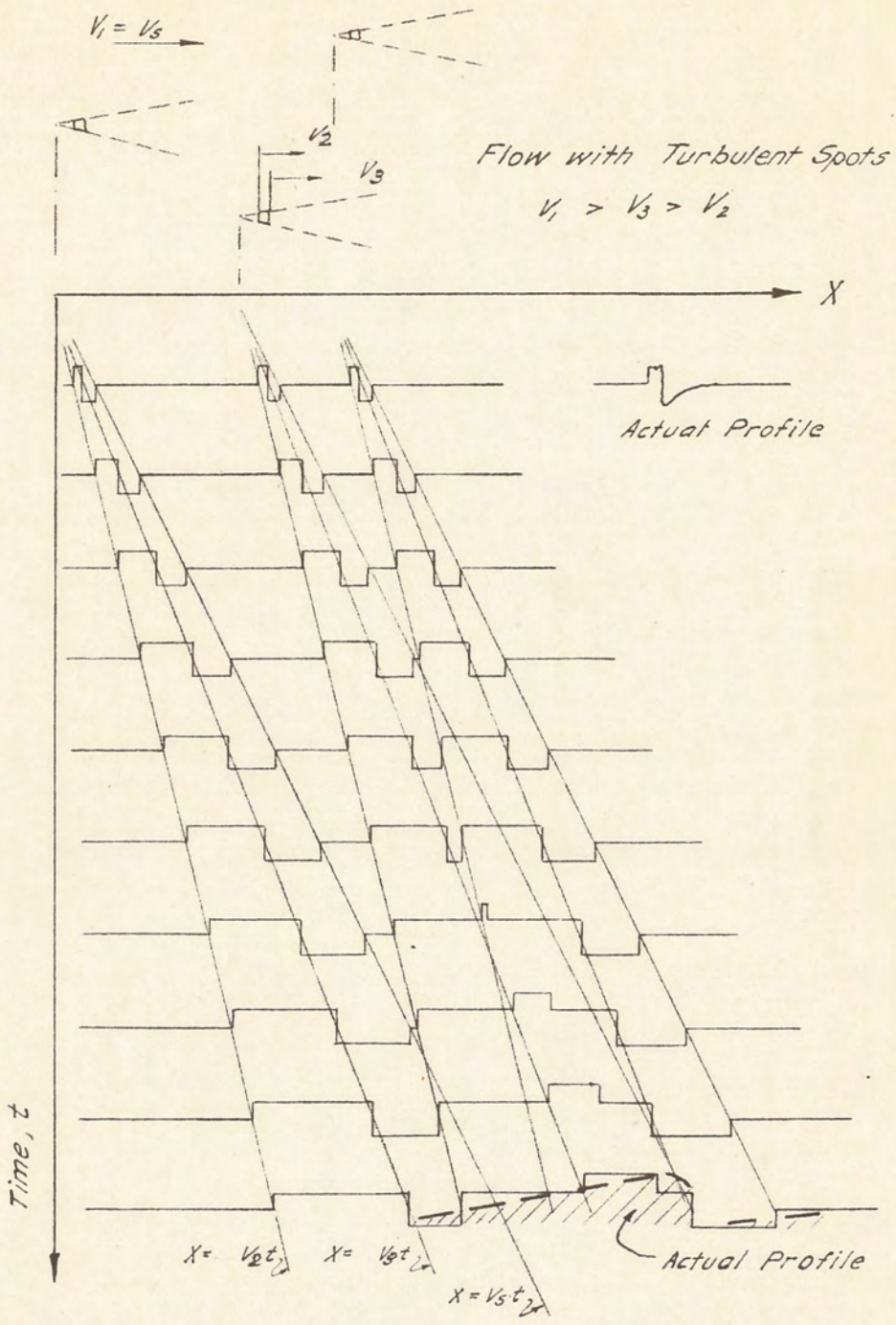

Fig. 9 t-X Diagram with Model of Slug Flow Development

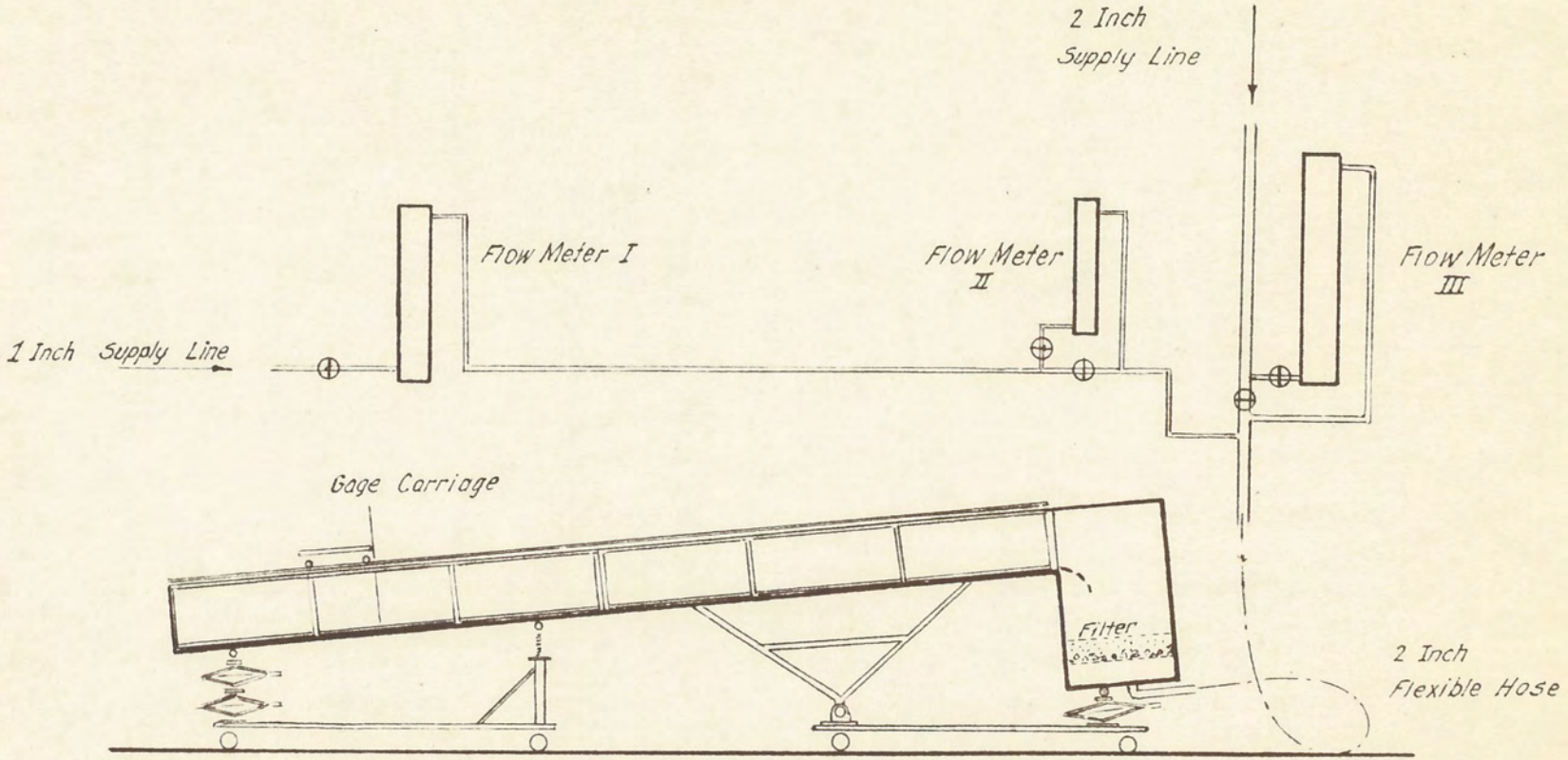

Fig. 10 Sketch of Laboratory Installation

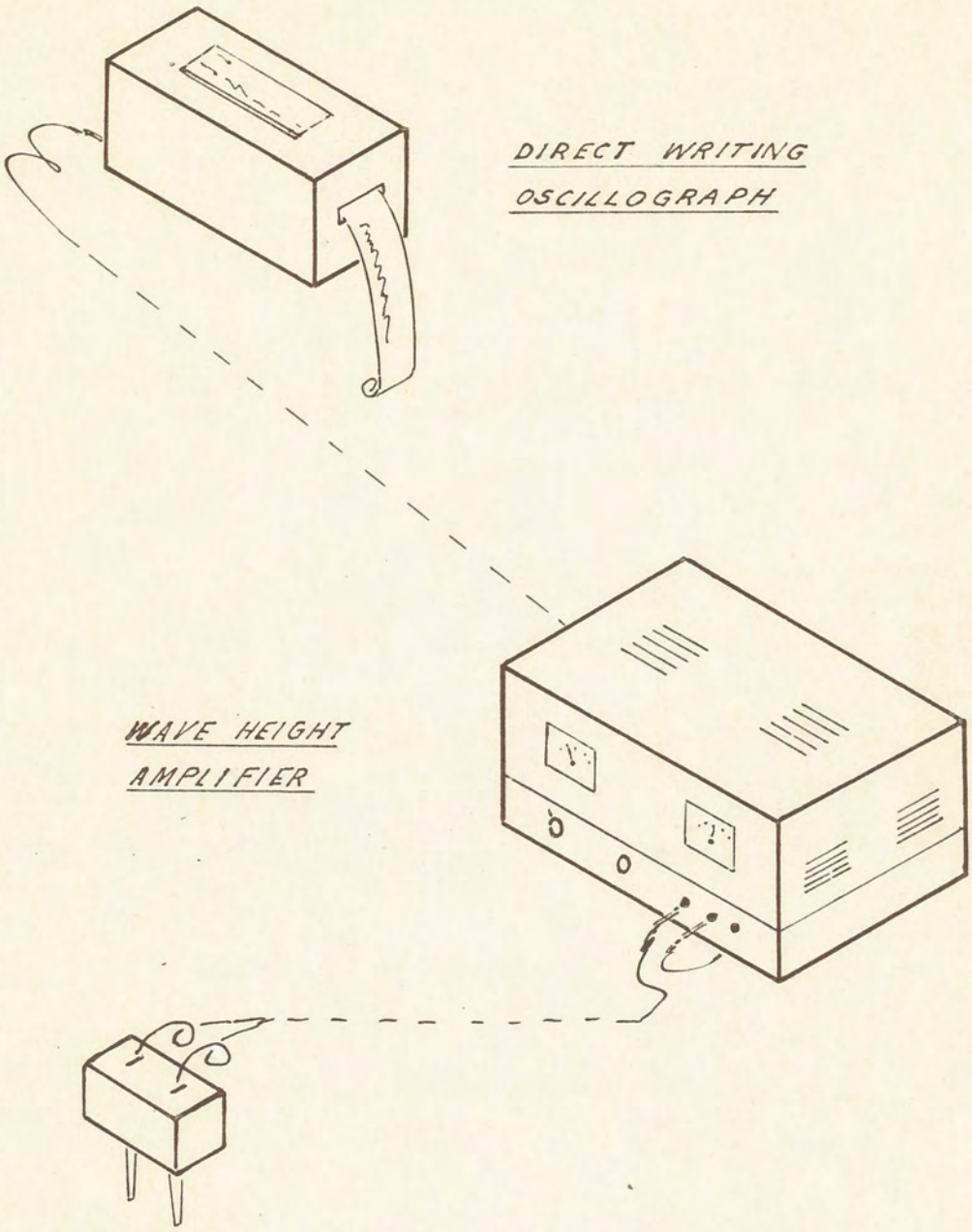

FIGURE 11 SCHEMATIC VIEW OF WAVE RECORDER

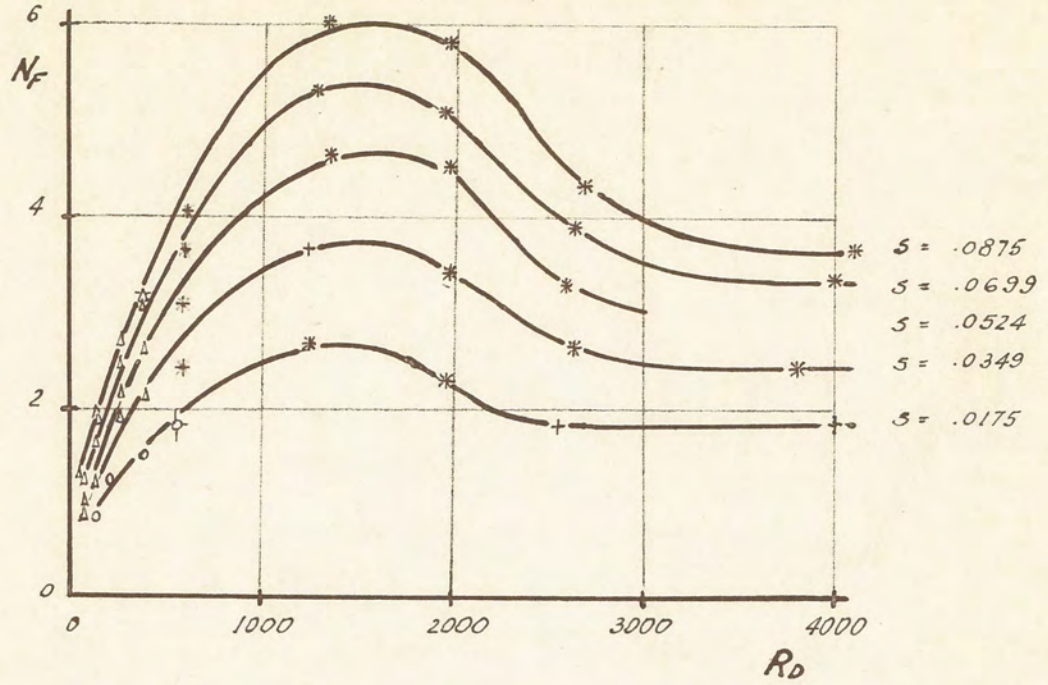

Fig. 12 Relation Between Froude and Reynolds Numbers at Various Slopes

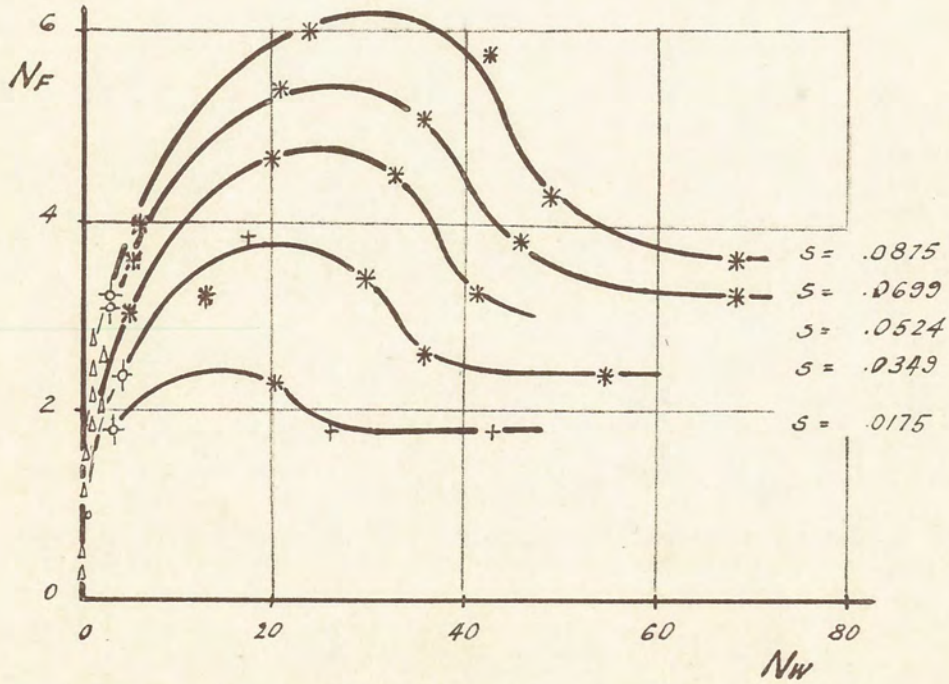

Fig. 13 Plot of Froude and Weber Numbers

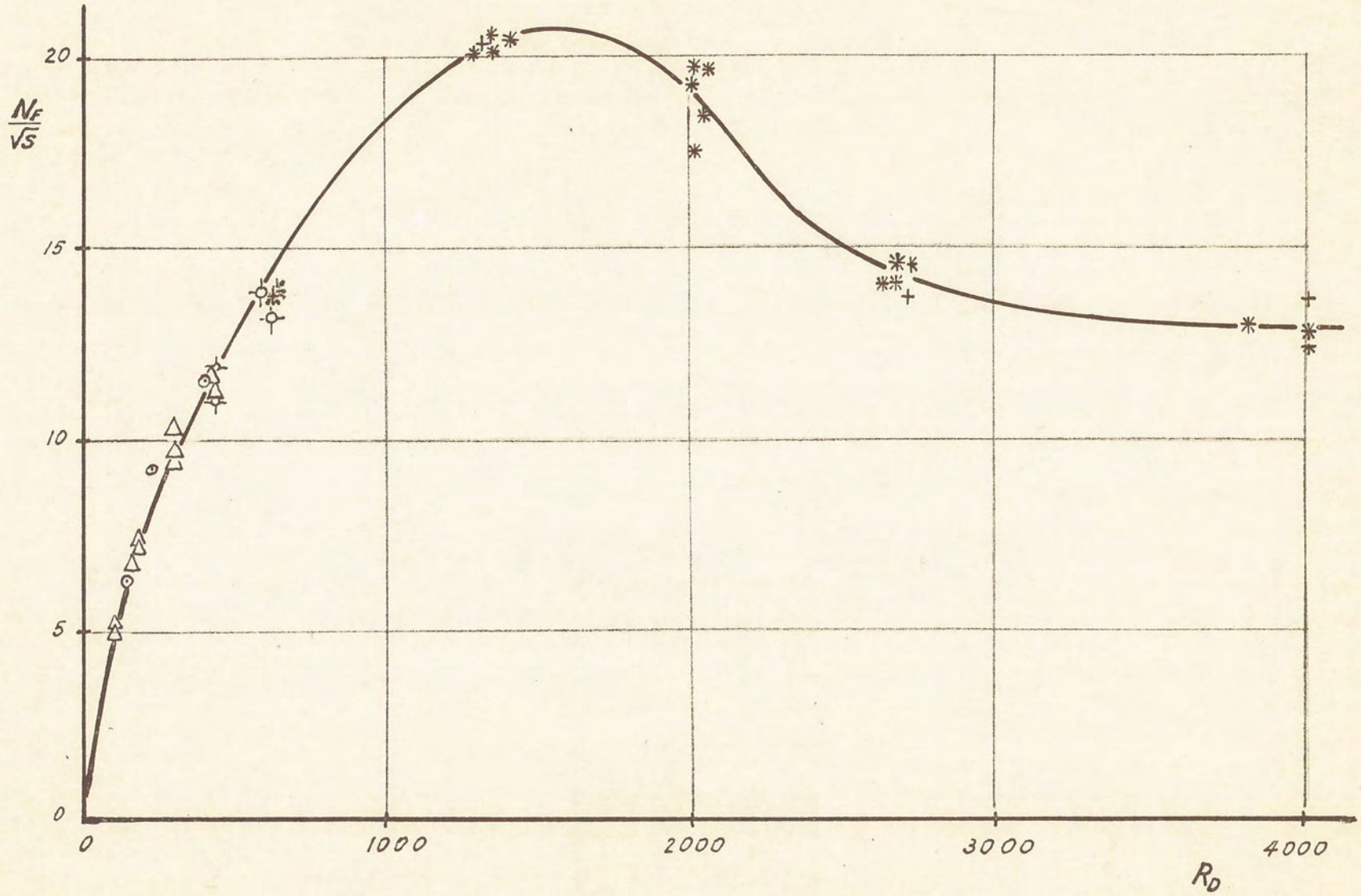

Fig. 14 Plot of Modified Froude Number and Reynolds Number

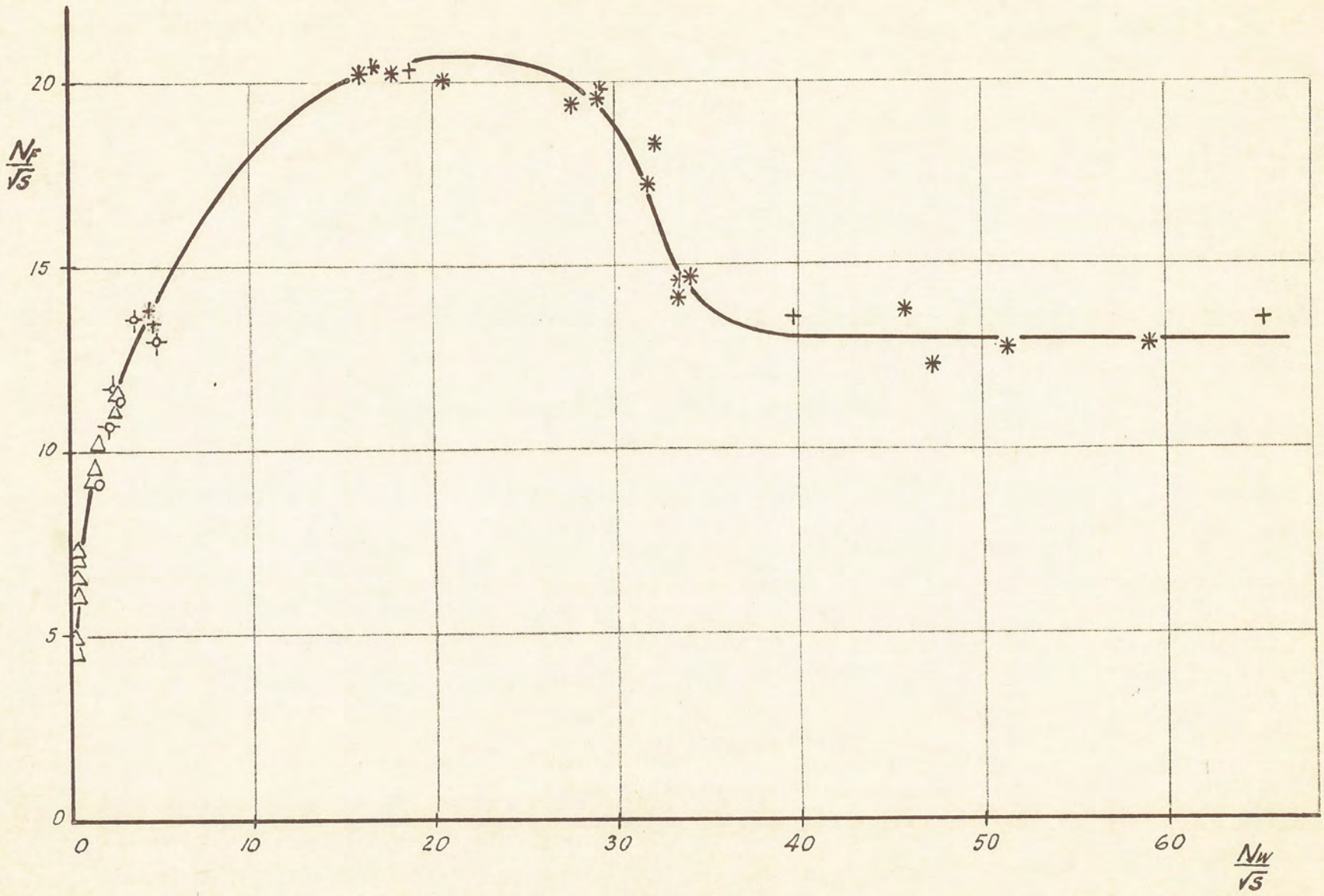

Fig. 15 Plot of Modified Froude and Weber Numbers

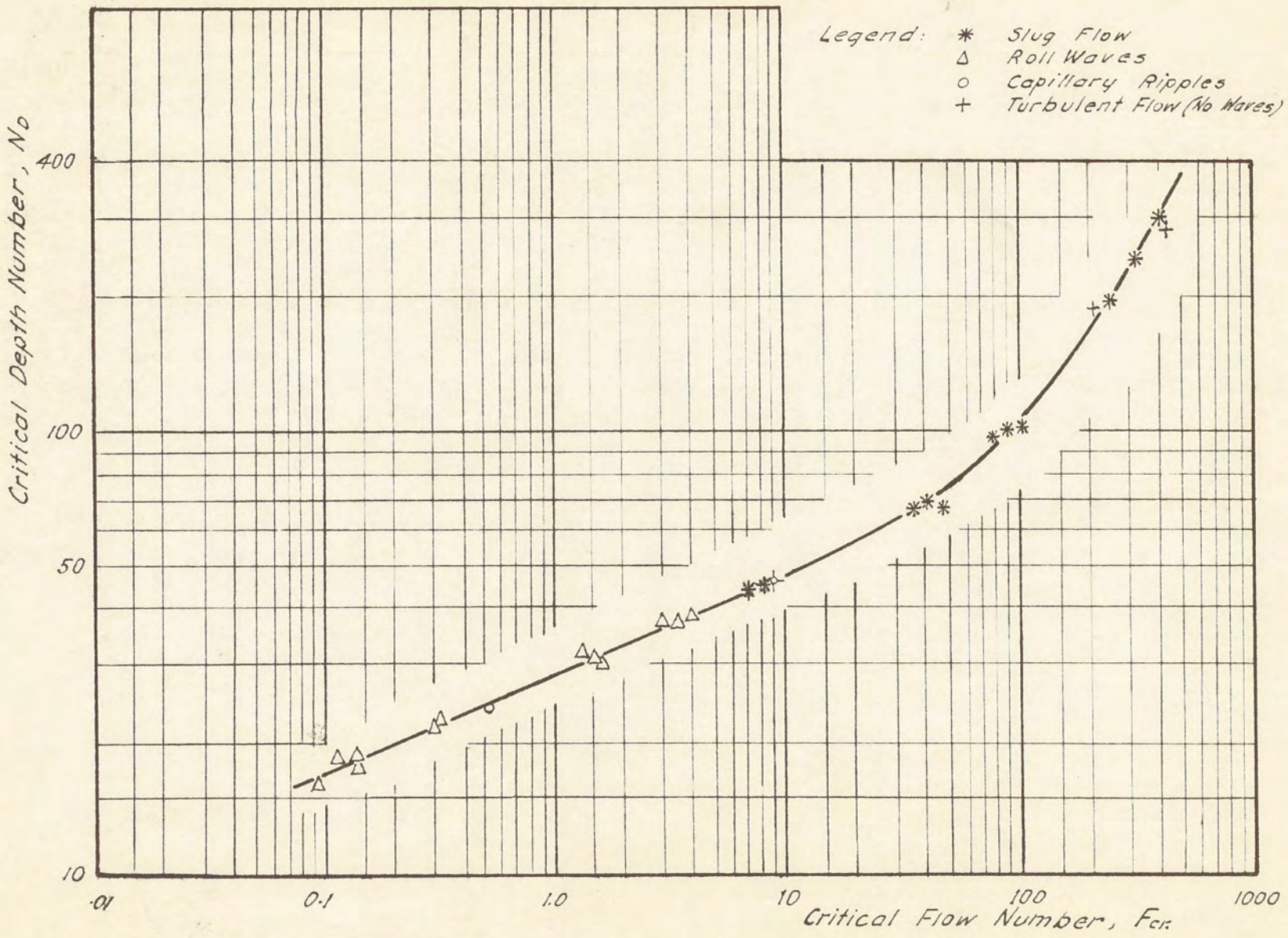

Fig. 16 Plot of Critical Depth and Critical Flow Numbers

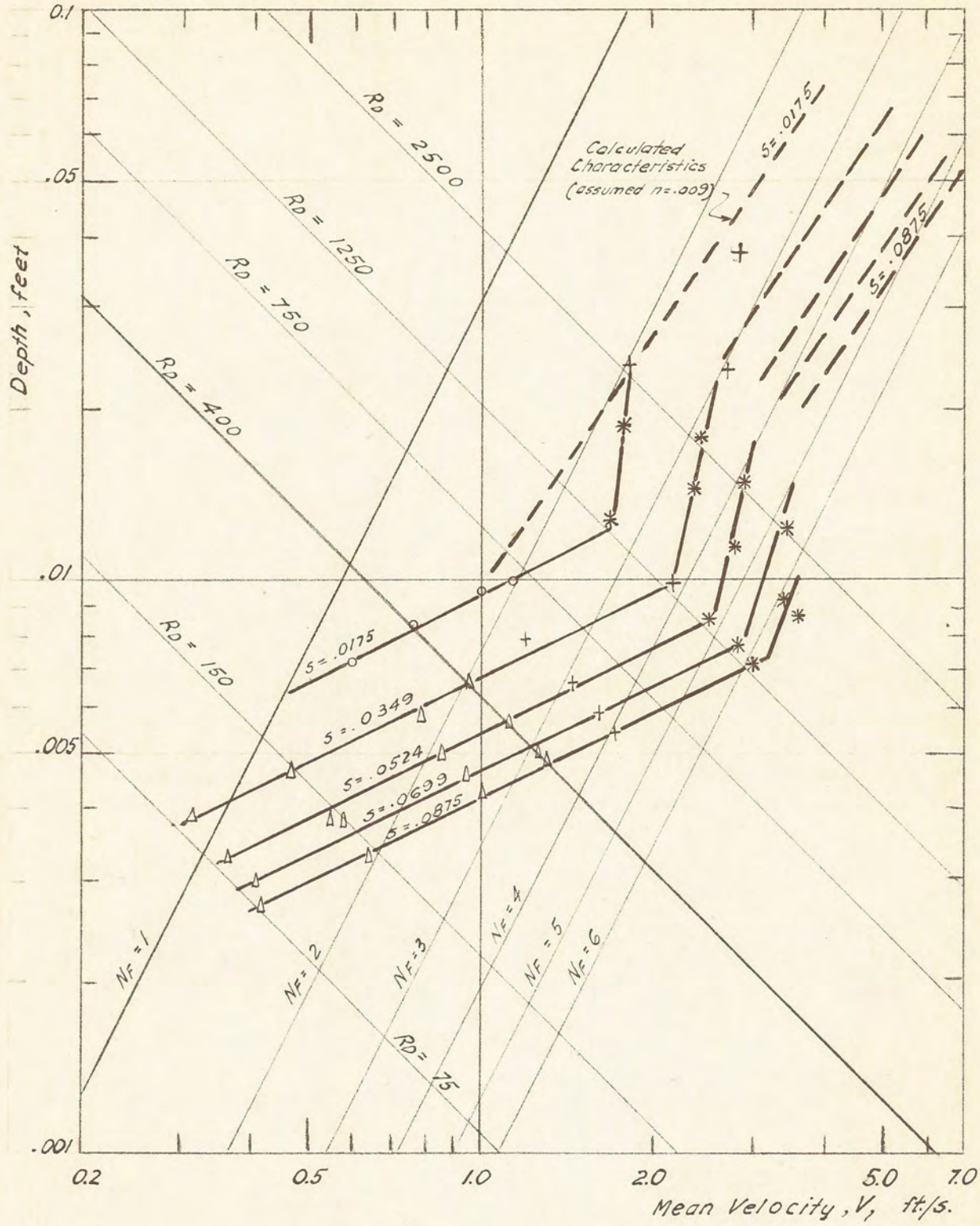

Fig. 17 Relations Between Depth and Velocity at Various Slopes for Flows in Laminar, Transitional and Turbulent Regions

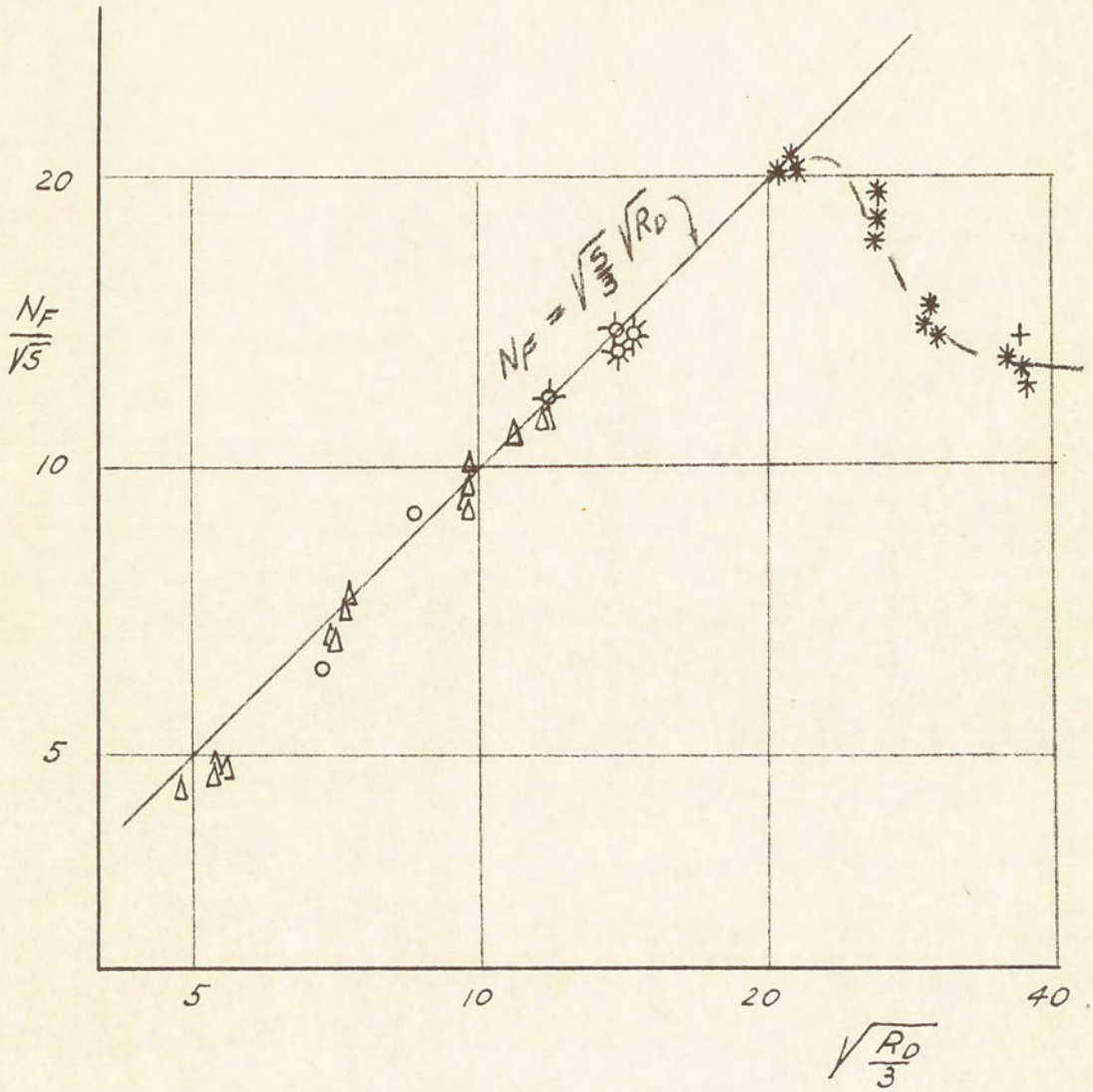

Fig. 18 Relationship Between Froude Number, Reynolds Number and Slope

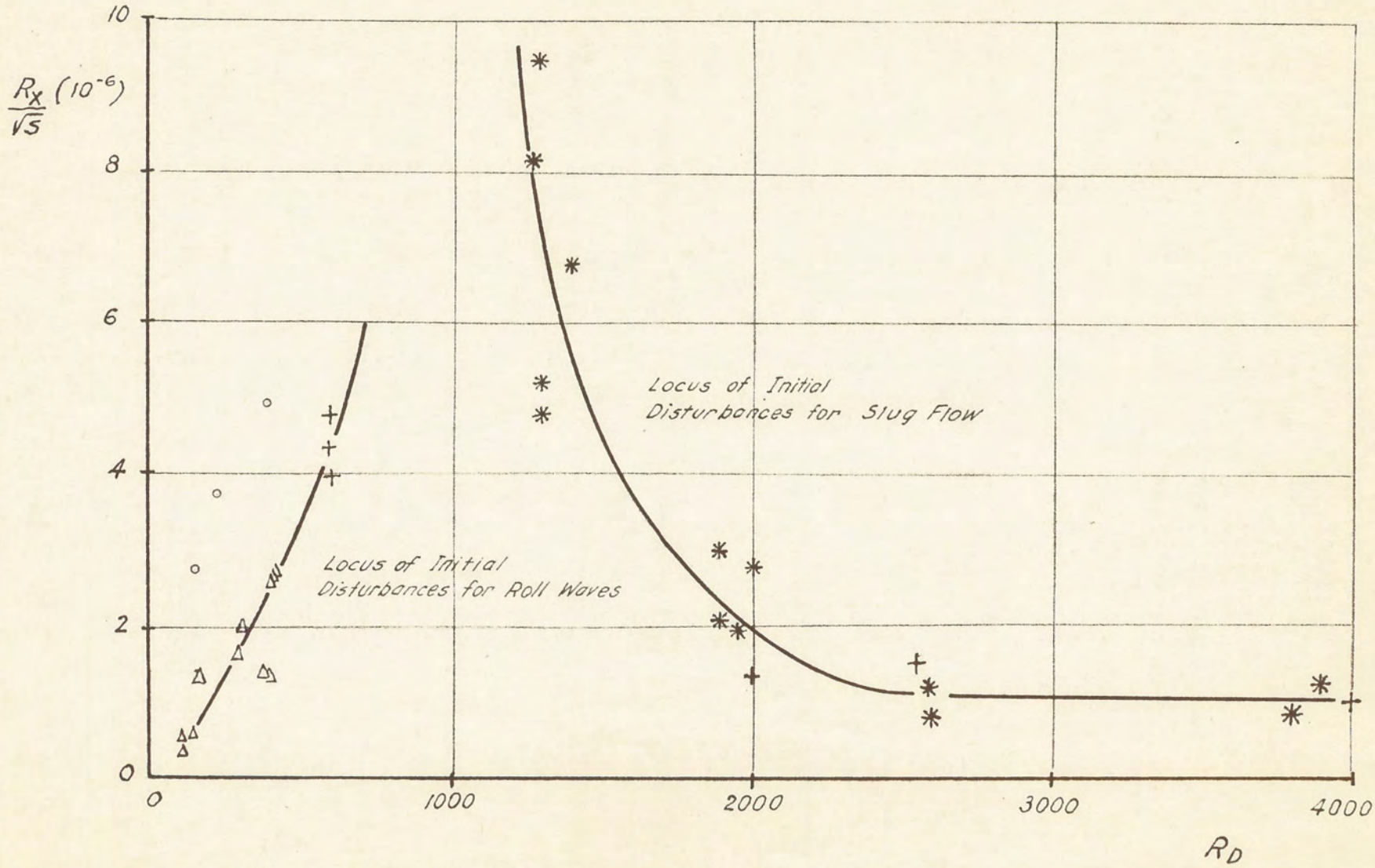

Fig. 19 Plot of Modified Length Reynolds Number and Depth Reynolds Numbers Showing Location of Initiation

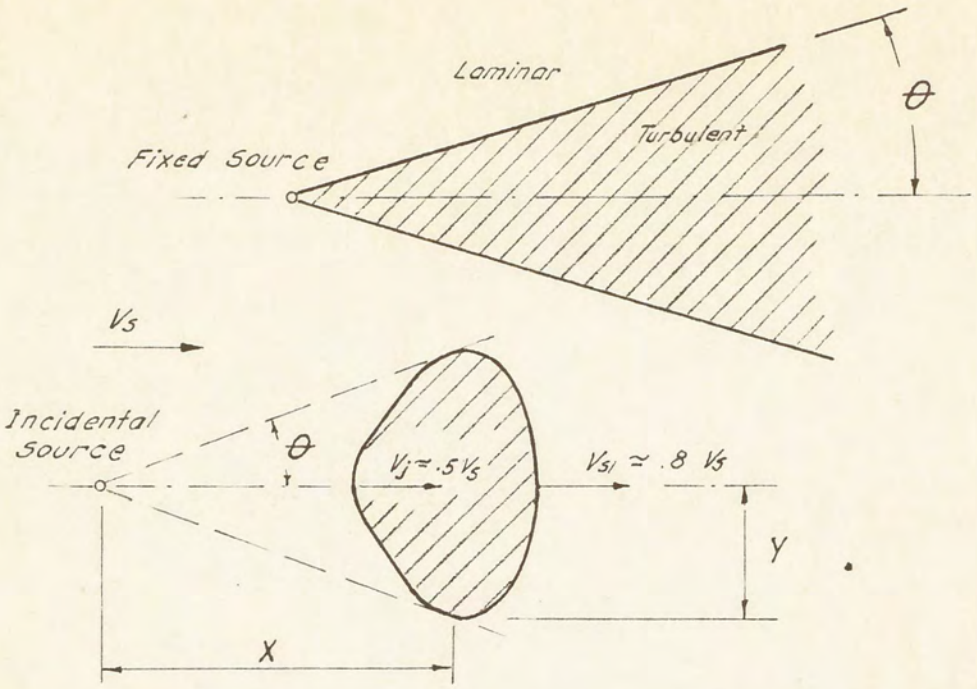

Fig. 21 Growth of Turbulent Spot

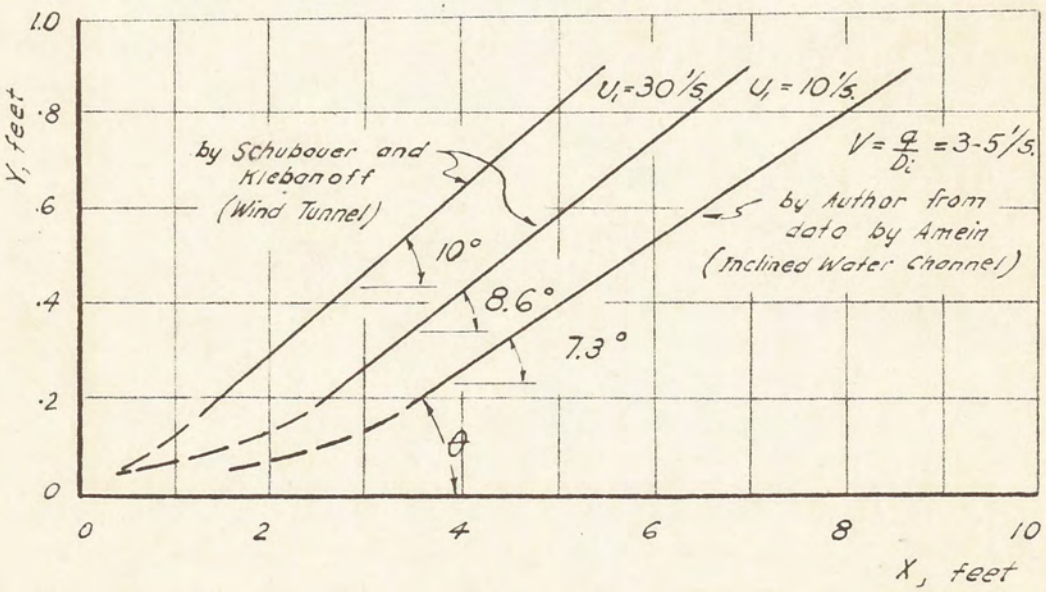

Fig. 22 Envelopes of Spot Growth

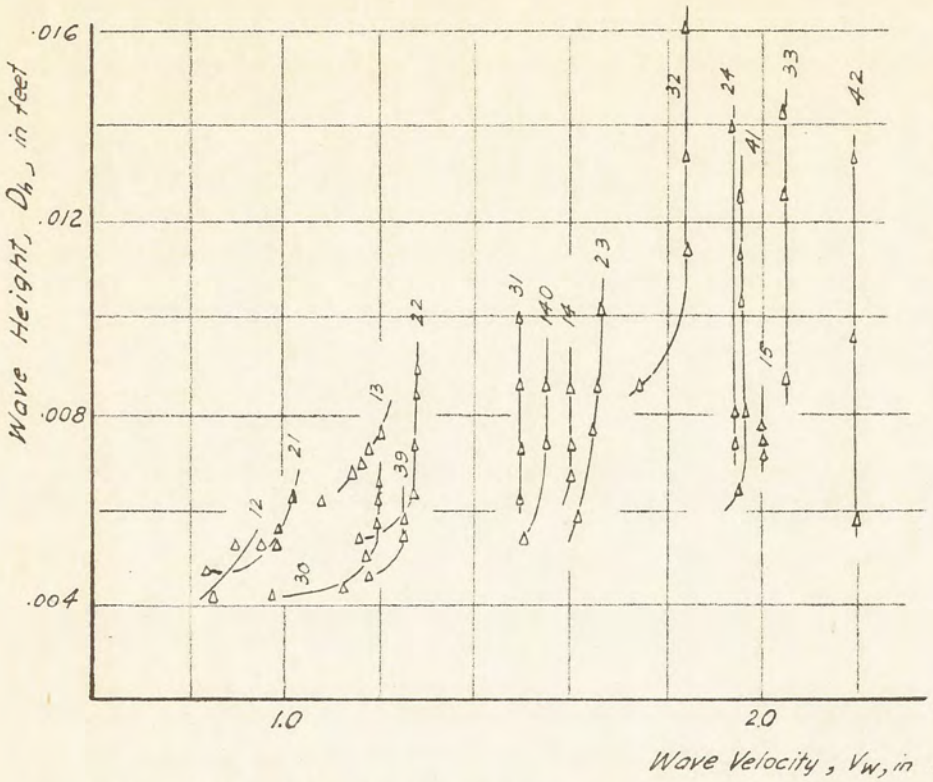

Run	Slope	R_D
12	.0349	84
13	"	151
14	"	286
15	"	410
21	.0524	87
22	"	157
23	"	286
24	"	413
30	.0699	91
31	"	159
32	"	290
33	"	419
39	.0875	74
40	"	149
41	"	288
42	"	418

Fig. 23 Relationship between Wave Height and Wave Velocity for Roll Waves

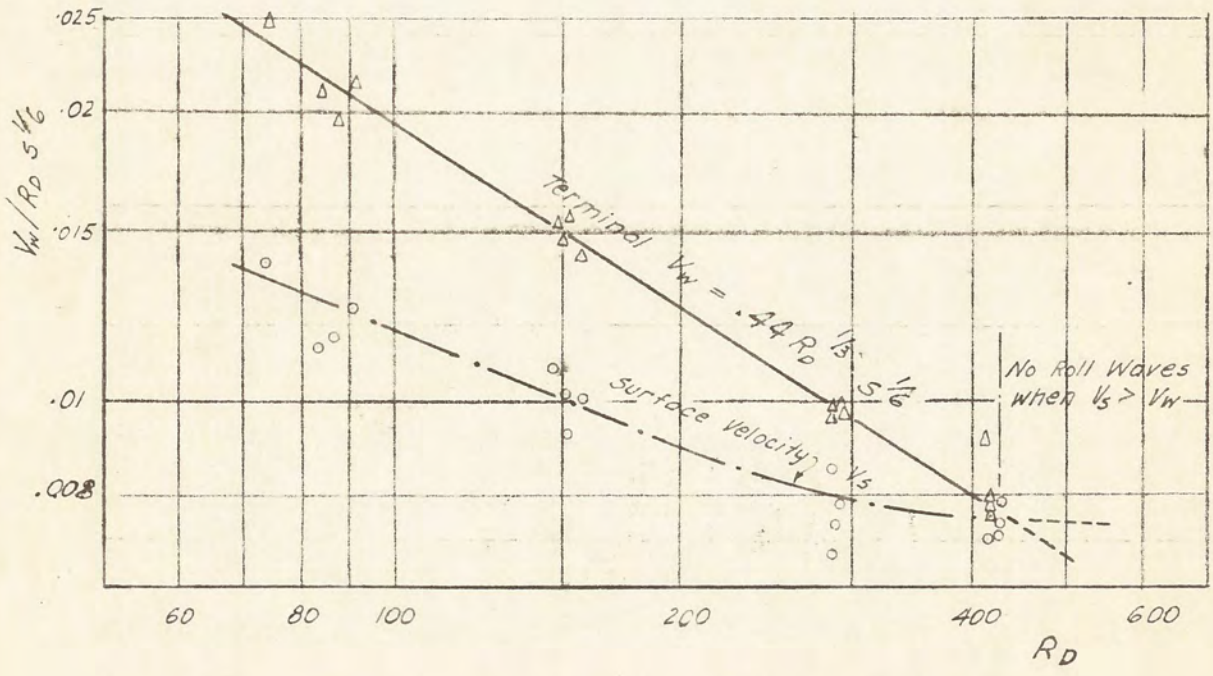

Fig. 24 Terminal Roll Wave Velocity as a Function of Reynolds Number and Slope

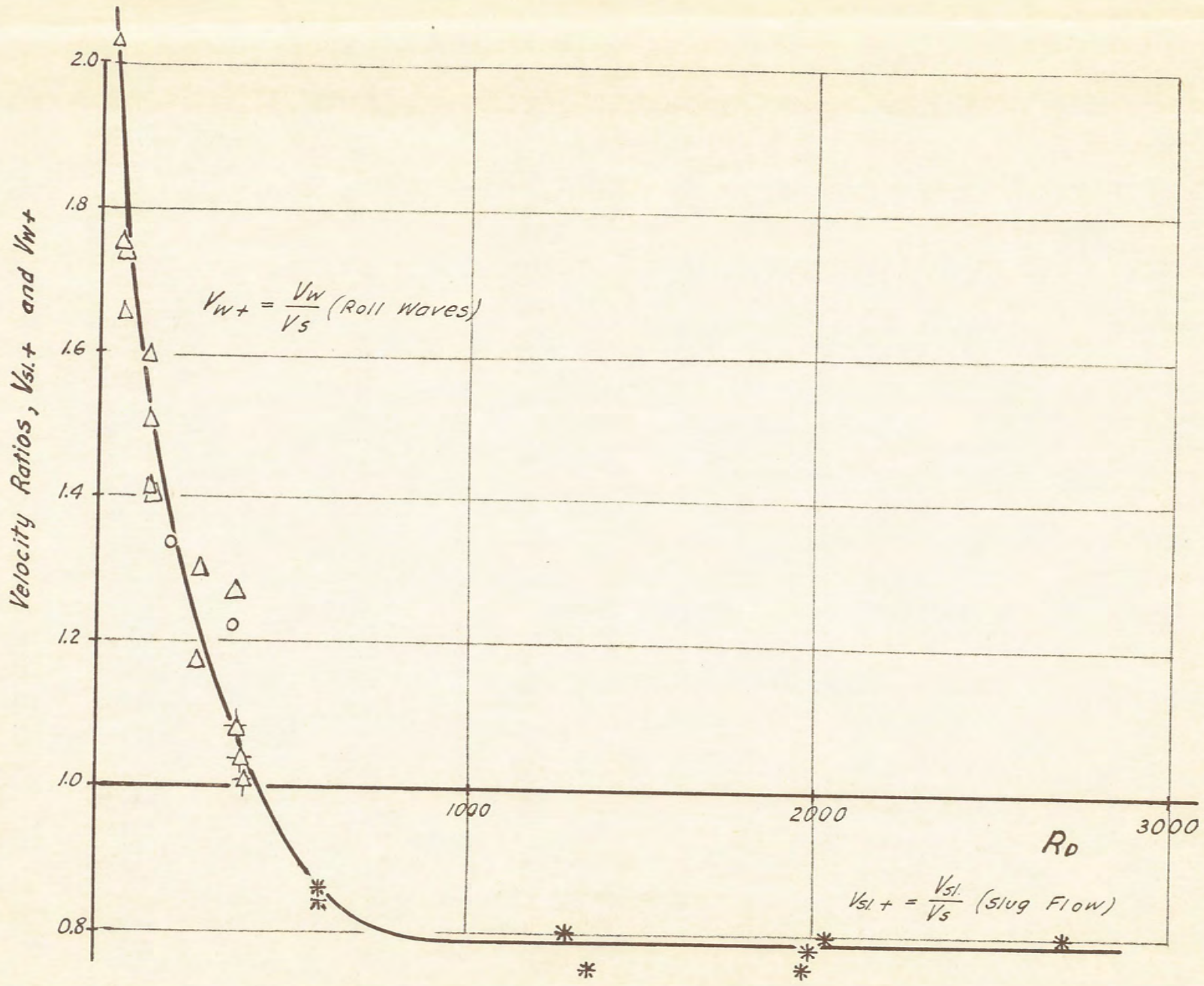

Fig. 25 Plot of Velocity Ratios and Reynolds Number at Station 23

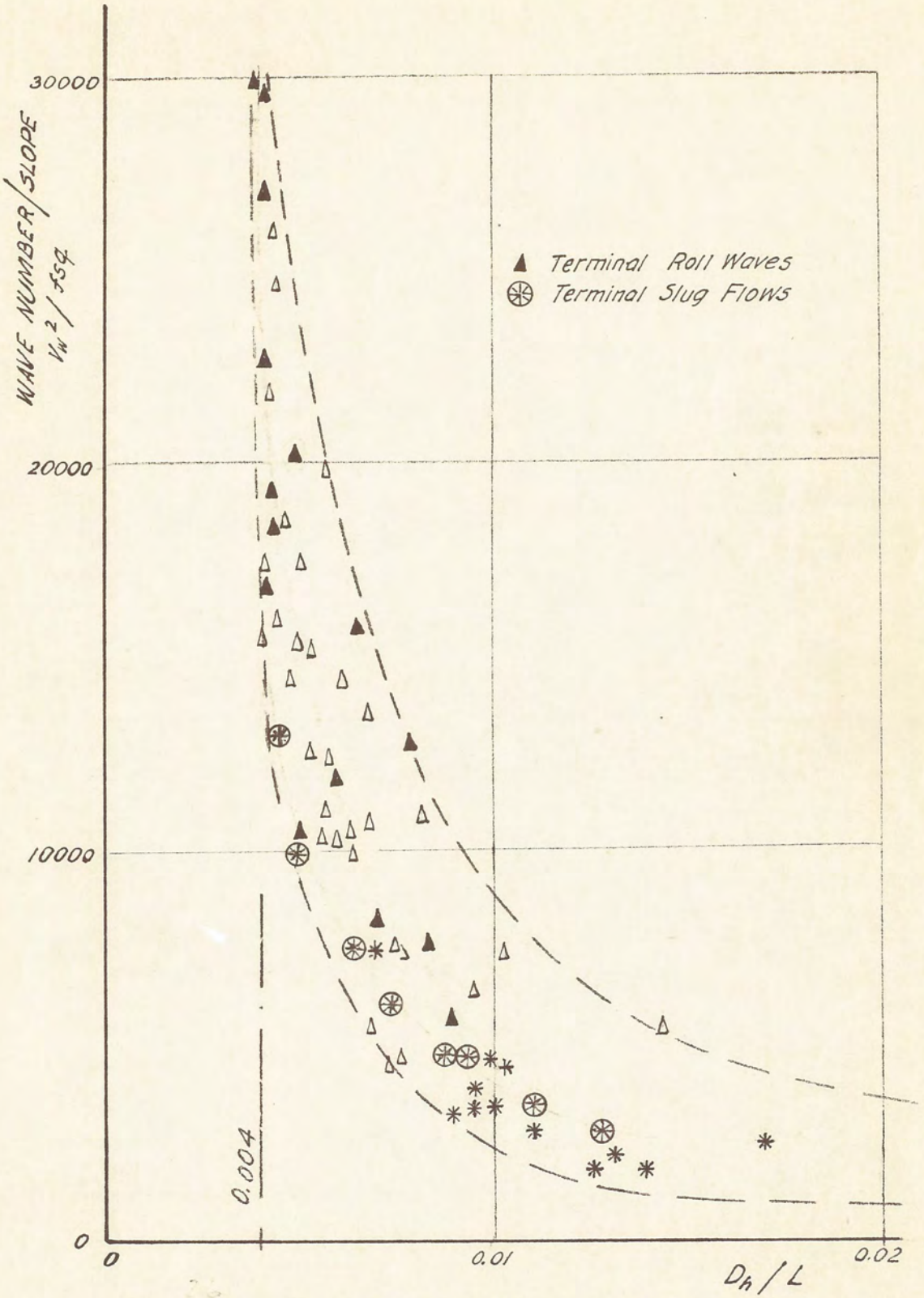

Fig. 26 Plot of Modified Wave Number and Ratio of Wave Height to Wave Length